Studies on Higgs Boson Yukawa Couplings and Self-coupling at ATLAS

刘彦麟

密歇根大学

北京大学高能物理中心学术报告

Outline

- General introduction
- CP Property of the Top-quark Yukawa Coupling via ttH/tH (H→$\gamma\gamma$): Yukawa coupling to 3rd generation fermion
- Search for SM H→μμ: Yukawa coupling to 2nd generation fermion
- HH→bb$\tau\tau$ and HH combination: Higgs boson trilinear self coupling

Standard Model

- A theoretical framework to describe the elementary particles and their interactions
- The cornerstones of the SM:
  - ➢ Gauge invariance (based on SU(3)×SU(2)×U(1)): depicting strong and electroweak interactions
  - ➢ Higgs mechanism: trigger the EWSB; W, Z bosons and fermions acquire masses through EWSB; predicts the Higgs boson

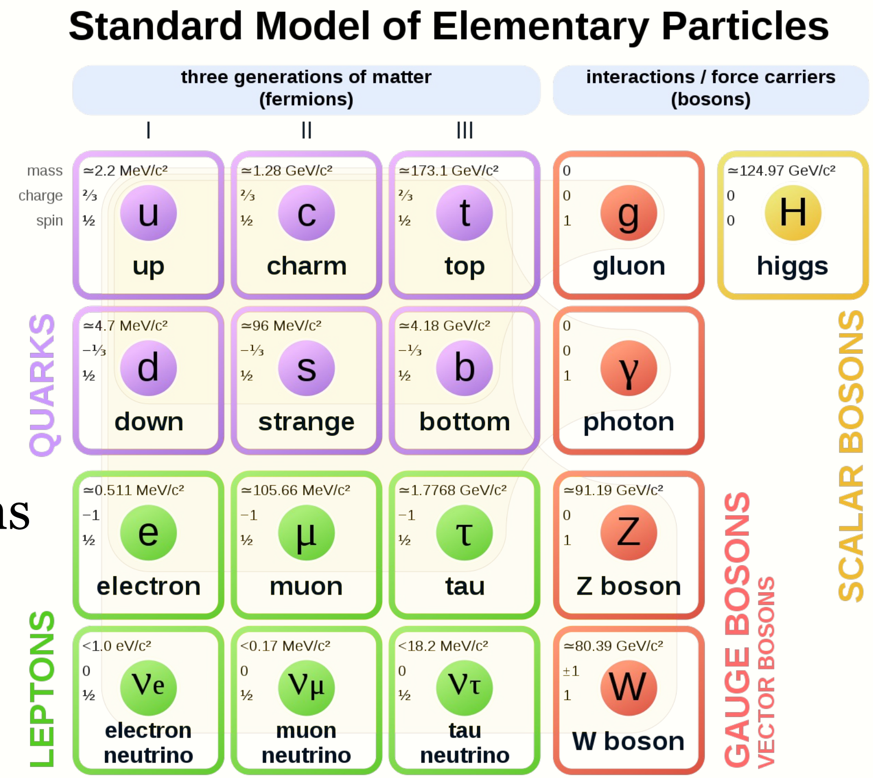

Higgs boson discovered in 2012

F. Englert and P. Higgs won the Nobel prize in 2013

Higgs Boson

- SM Higgs boson: $J^{CP} = 0^{++}$; neutral charge
- The measured mass: 125.09 ± 0.24 GeV (Run 1 ATLAS+CMS)

Higgs boson production at the LHC

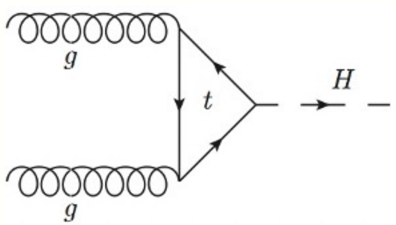

gluon-gluon Fusion (ggF): 48.5 pb

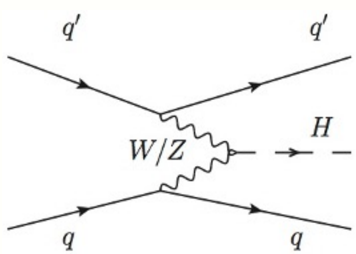

Vector Boson Fusion (VBF): 3.8 pb

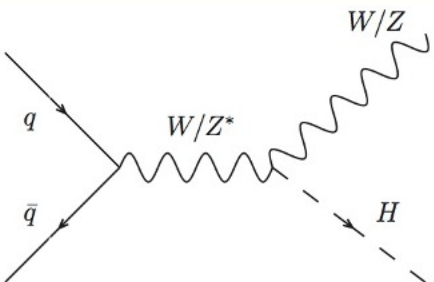

Associated production with vector boson (VH): 2.3 pb

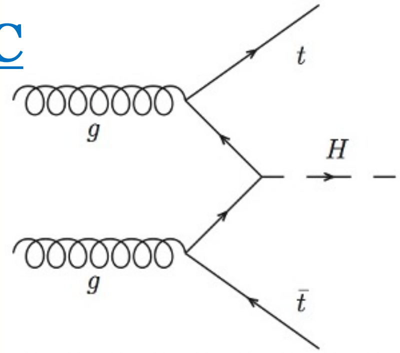

Associated production with top quark pair (ttH): 0.5 pb

Since the discovery of the Higgs boson, measuring its property and coupling can be used as an approach to probe new physics beyond the SM, source of matter-antimatter asymmetry, etc

Yukawa Couplings and Self-coupling

- Higgs boson couples to fermions through Yukawa interactions
  - ➢ Giving masses to quarks and leptons
  - ➢ Coupling strength is proportional to fermion's mass
- Higgs potential: $V(\phi) = \mu^2 \phi^\dagger \phi + \lambda(\phi^\dagger \phi)^2$
  - ➢ In SM, $\lambda \approx 0.13$ give $m_H \approx 125$ GeV
- HH productions provide directly access to Higgs self-coupling κ_λ ($\lambda_{HHH}/\lambda_{SM}$)

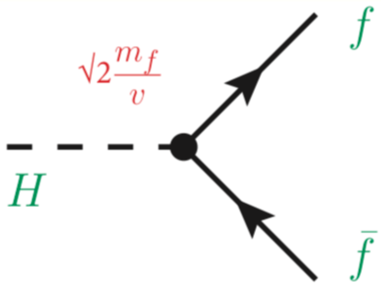

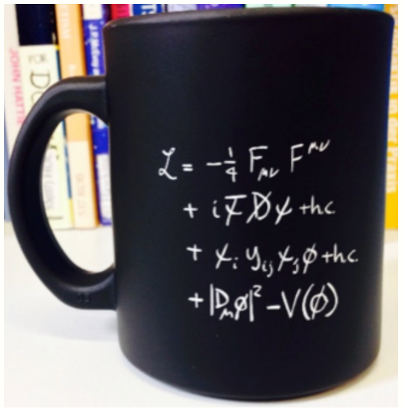

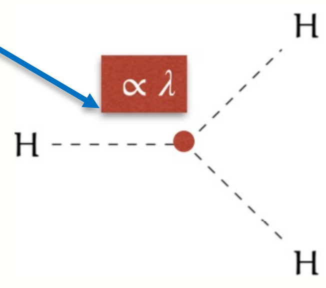

ATLAS Detector

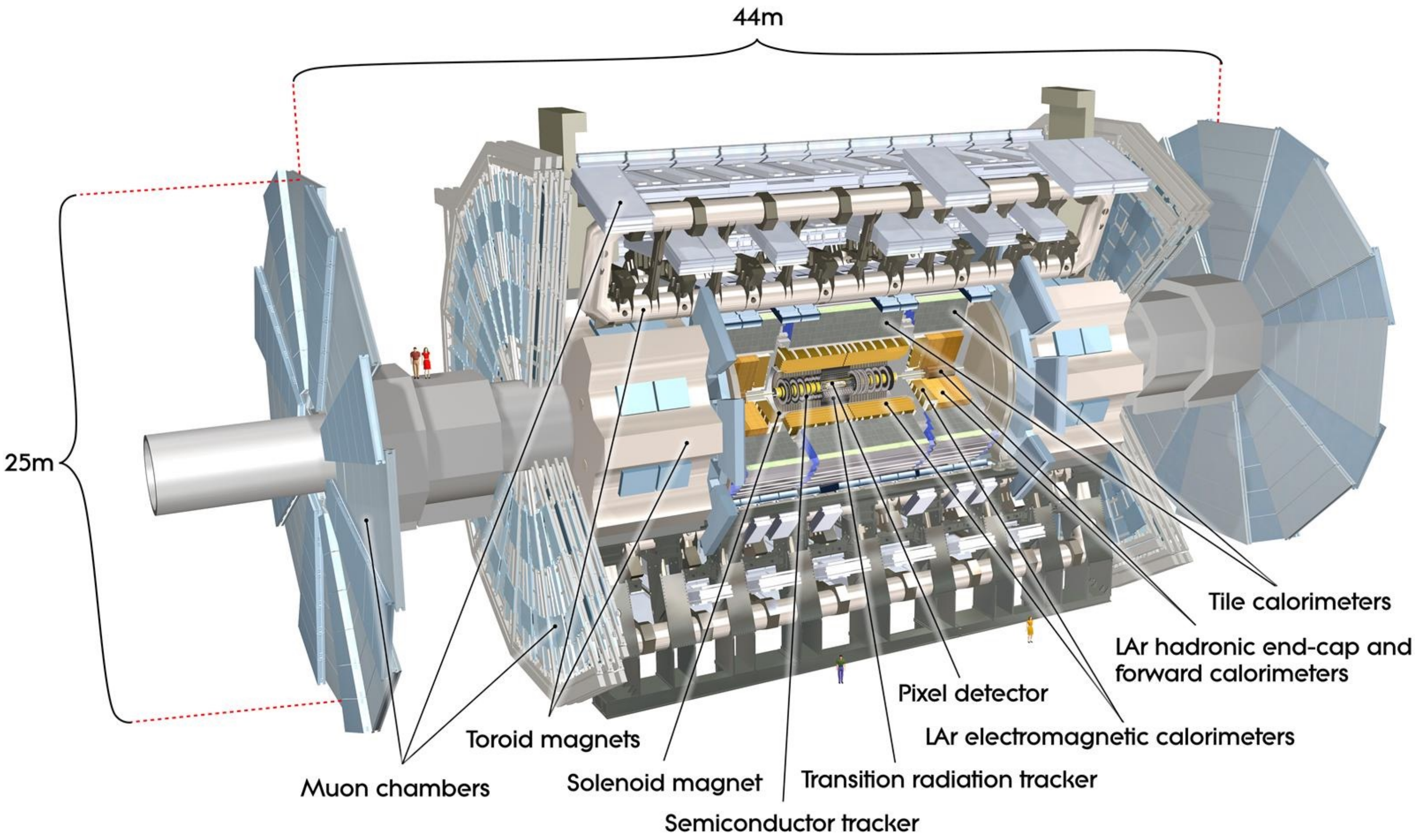

Run 2 Dataset

- 139 fb^{-1} of 13 TeV pp collision data collected for physics by the ATLAS detector during the LHC Run 2
- Great performance of ATLAS detector and operation of the LHC

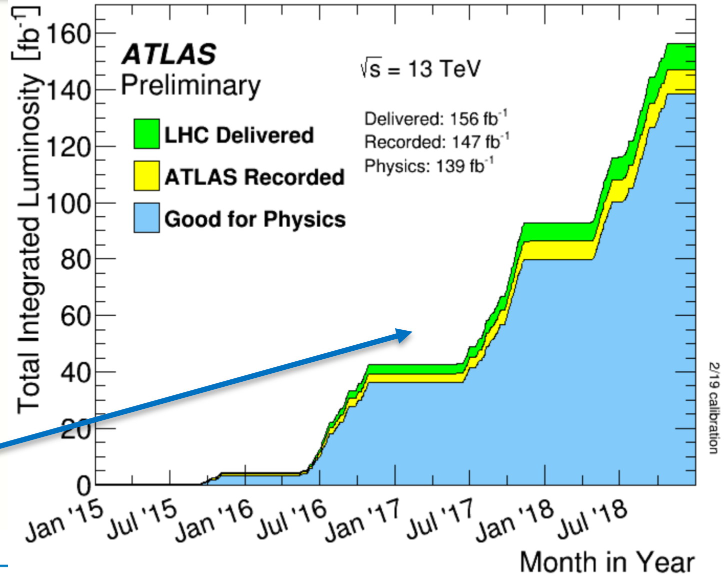

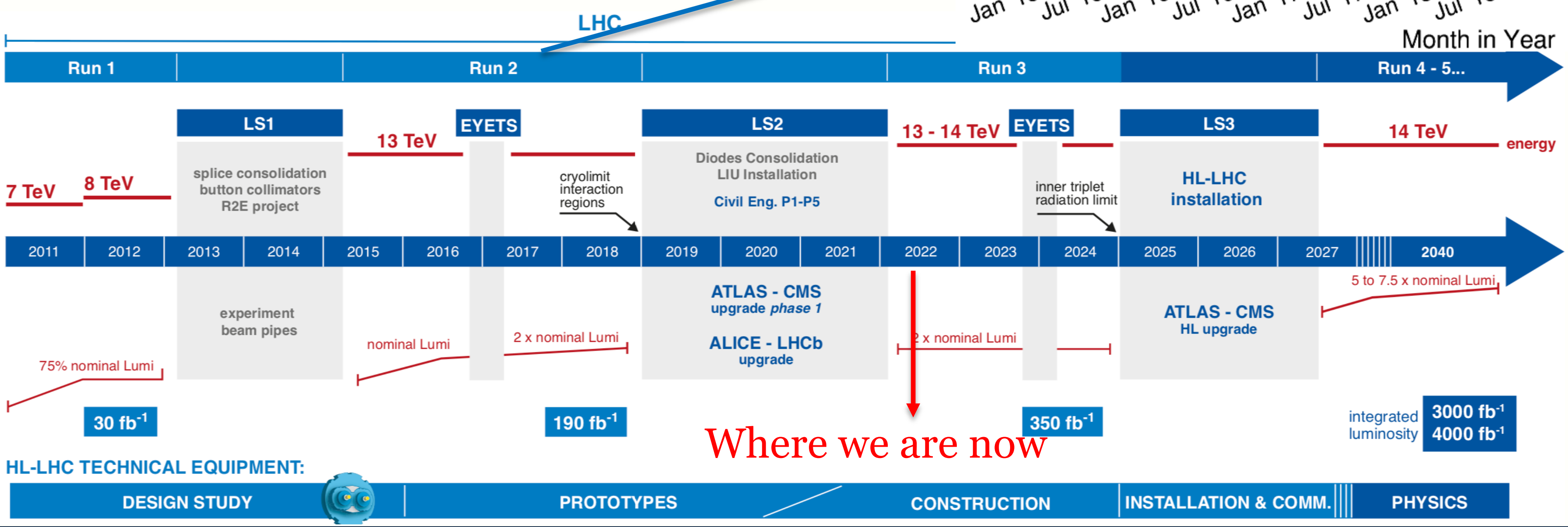

CP Property of the Top-quark Yukawa Coupling via ttH/tH ($H \rightarrow \gamma\gamma$)

Why Doing This?

- Large matter-antimatter asymmetry in universe: crucial to look for additional CP violation sources
- First direct probe to the CP property of the top-Higgs Yukawa coupling (referred as t-H coupling later) using ttH and tH
  - Lagrangian written as: $\mathcal{L} = -\frac{m_t}{v}\left\{\bar{\psi}_t \kappa_t \left[\cos(\alpha) + i\sin(\alpha)\gamma_5\right]\psi_t\right\} H$
  - κ_t (>0): coupling strength; α: CP-mixing angle
  - In SM, $\kappa_t = 1$, $\alpha = 0$
- Any deviation observed can be a sign of new physics and account for the explanation of the observed matter-antimatter asymmetry

How to Probe this?

- The presence of a CP-odd component in the t-H coupling will have impact on
  - rate and kinematics of ggF process
  - rate of H→$\gamma\gamma$ decay
  - rate and kinematics of ttH and tH processes

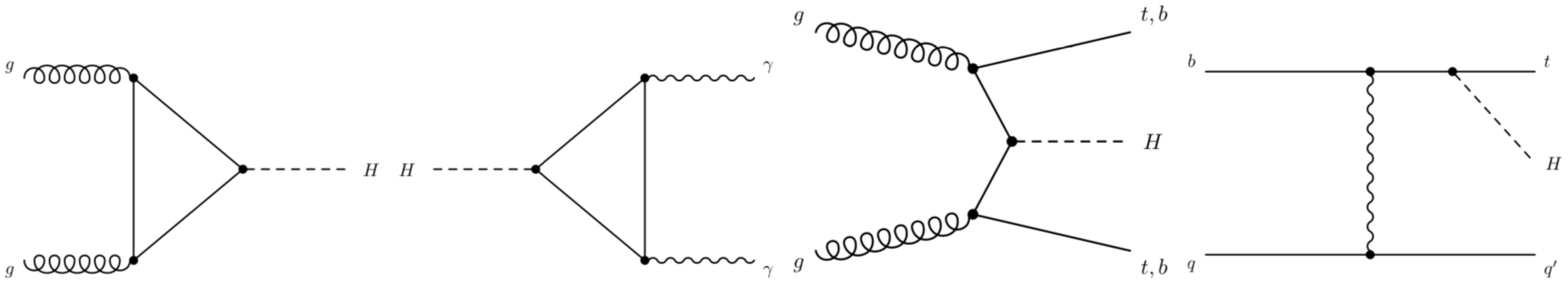

- Measure the rate of ttH/tH processes and shapes of observables sensitive to the CP nature of the t-H coupling
  - Contributions from ggF and H→$\gamma\gamma$ constrained by the Higgs combination results

Why in H→$\gamma\gamma$ Channel?

- $\gamma\gamma$ channel: small rate, but clean signature and good resolution; solid background estimation from data sideband
- $\gamma\gamma$ selection: two isolated photons with $p_T > 35/25$ GeV; 105 GeV < $m_{\gamma\gamma}$ < 160 GeV (fitting discriminant)
- ttH/tH selection: ≥1 b-tagged jet (77% eff.)
  - ”Lep” region (≥1 W decay leptonically): ≥ 1 isolated electron or muon with $p_T > 15$ GeV
  - “Had” region (both tops decay hadronically): 0 selected lepton, ≥ 3 jets

BDT Methodology

- Selected events are categorized based on a two-dimensional BDTs
- "Background Rejection BDT": trained to separate ttH-like events from $\gamma\gamma$+jets and tt$\gamma\gamma$ background
- "CP BDT": trained to separate CP-even and CP-odd couplings using ttH and tH processes
- Training variables include p_T and η of $\gamma\gamma$ system and two top candidates (t1, t2); angular variables $\phi_{\gamma\gamma,t1}$ and $\phi_{\gamma\gamma,t2}$; angular separation variables $\Delta\eta_{t1t2}$ and $\Delta\phi_{t1t2}$; $m_{\gamma\gamma, t1}$, m_{t1t2}, etc

Event Categorization

- Categorization is done in Had and Lep regions separately

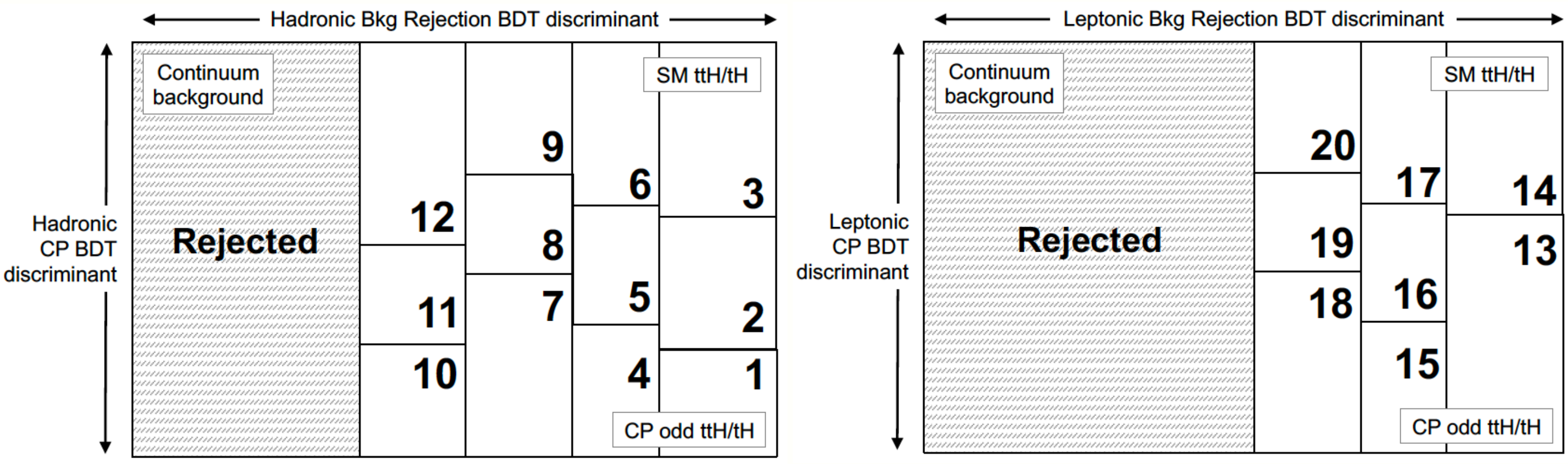

- The boundaries are chosen to achieve a strong separation between CP-even and CP-odd signals, as well as a good sensitivity to ttH process

Signal and Background Modeling

- Total background includes resonant background (non-ttH Higgs) and continuum processes
- Signal and resonant background modeled by the double-sided crystal ball functions
- Continuum background modeled by one-parameter functions
  - ➢ Exponential function: $f(m_{\gamma\gamma}) = e^{c \cdot m_{\gamma\gamma}}$
  - ➢ Power Law function: $f(m_{\gamma\gamma}) = m_{\gamma\gamma}^{c}$

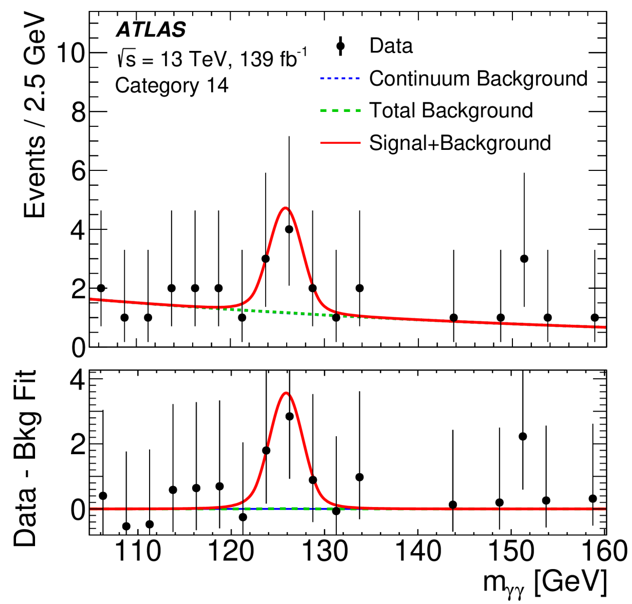

→ Choice based on $tt\gamma\gamma$ sample by applying stringent criteria on potential biases in the extracted signal yields

Significance for ttH(→$\gamma\gamma$)

- Assuming CP-even coupling, the measured signal strength ($\mu=\sigma_{obs}/\sigma_{SM}$) for ttH via H→$\gamma\gamma$ is:

$$\mu = 1.43\ {}^{+0.33}_{-0.31}(stat.)\ {}^{+0.21}_{-0.15}(sys.)$$

- The background-only hypothesis is rejected with an observed (expected) significance is 5.2σ (4.4σ)

The first time for ttH observation in single Higgs boson decay channel!

Results on CP-even and CP-odd

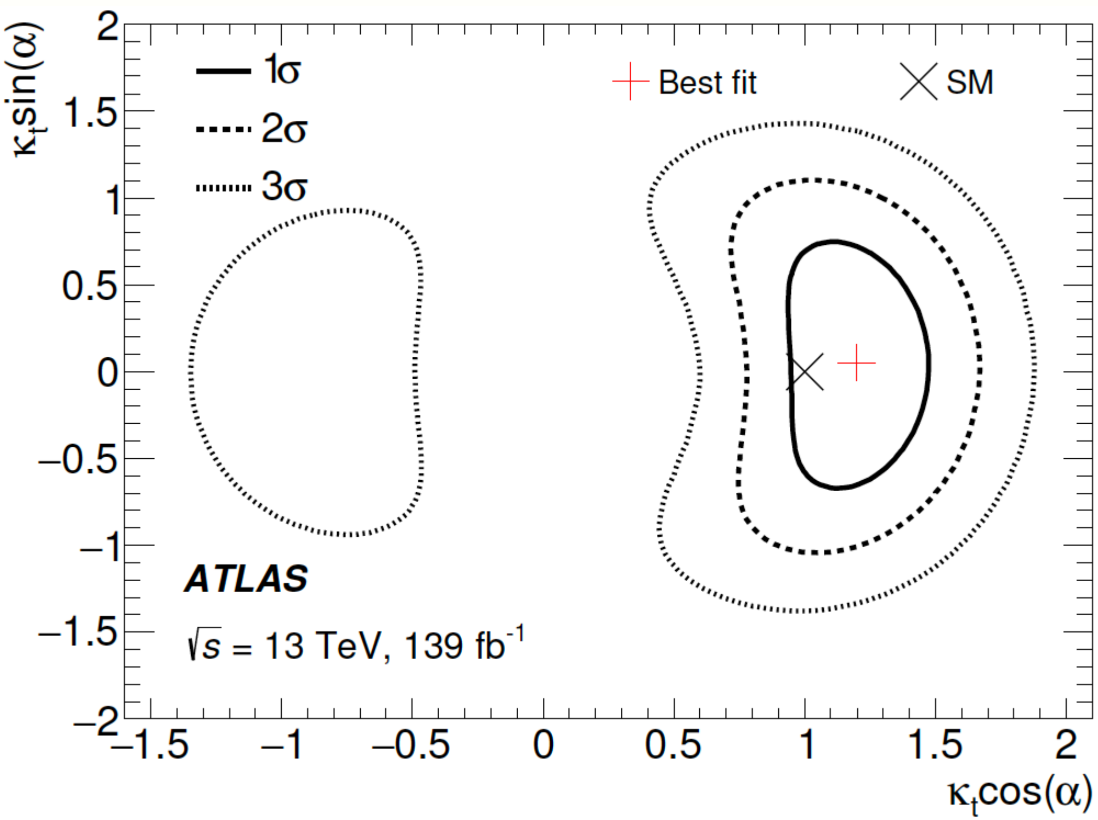

The measurements consistent with the SM prediction, and no sign of CP violation in the top-Yukawa interaction observed

Exclusions for CP-odd Component

- Likelihood scan of α with κ_t floating in the fit
- |α|>43° is excluded at 95% C.L.
- Pure CP-odd hypothesis is excluded at 3.9σ

The best exclusion result for CP-odd component search in the top-Yukawa interaction up to now!

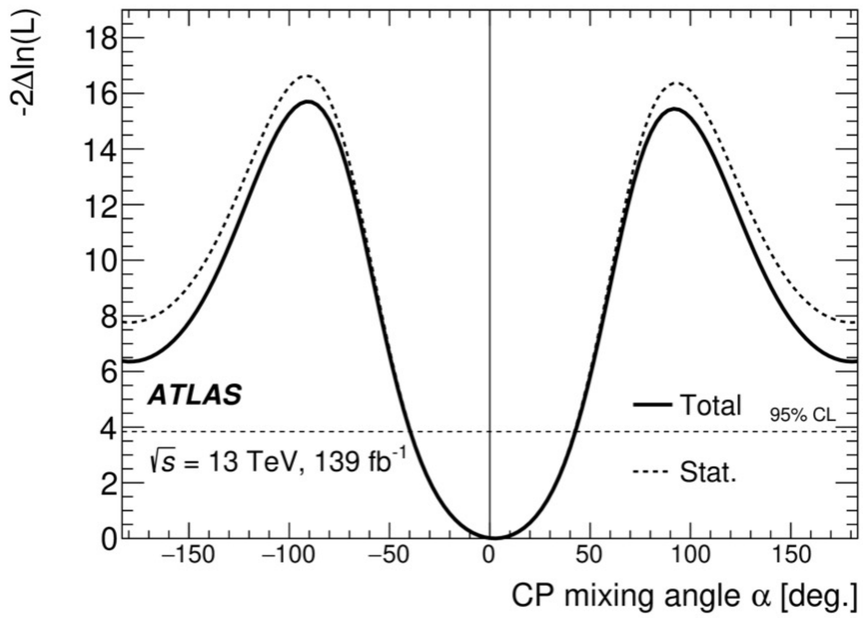

Ref.: Phys. Rev. Lett. 125 (2020) 061802

Reported by CERN Courier

CERNCOURIER | Reporting on international high-energy physics

Physics ▾ | Technology ▾ | Community ▾ | In focus | Magazine

HIGGS AND ELECTROWEAK | NEWS

First foray into CP symmetry of top-Higgs interactions

4 May 2020

Search for SM $H \rightarrow \mu\mu$

Physics Motivation

- H→μμ: most promising channel to explore Yukawa coupling to the 2nd generation of fermions
  - ➢ H→cc not very sensible under the current luminosity
- Major challenge for H→μμ: low branching ratio and large irreducible background from Drell-Yan

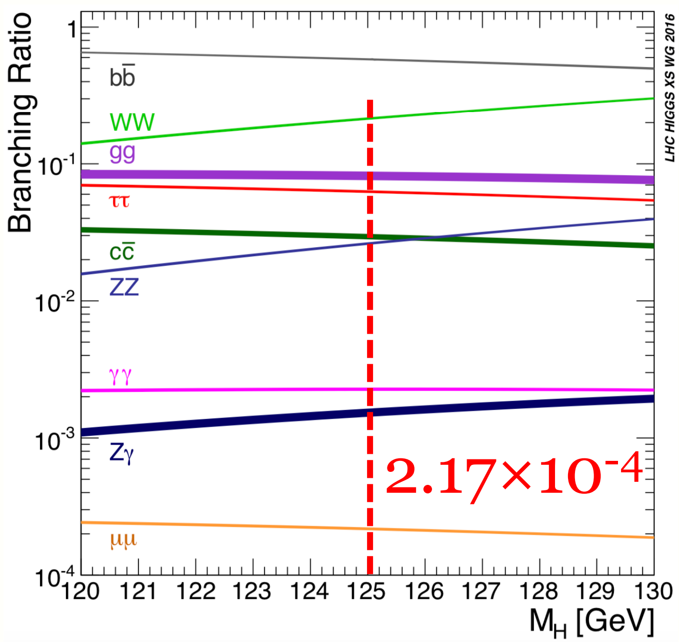

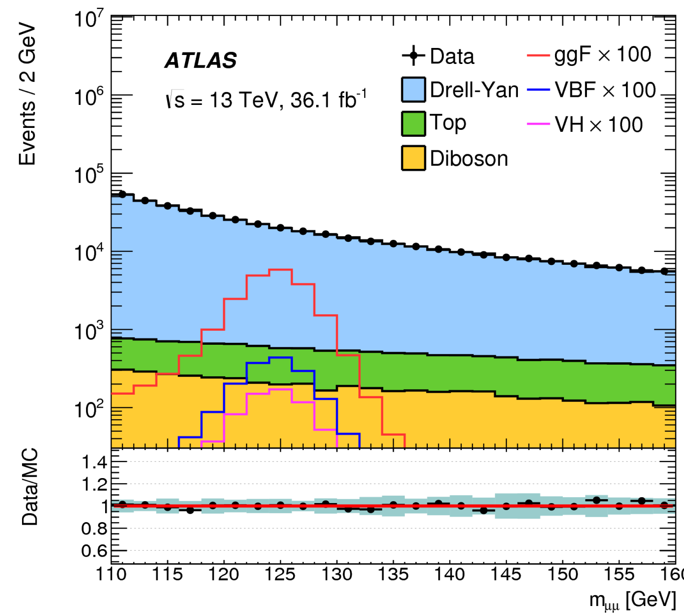

S/B: ~0.1%

Overview of Analysis Methodology

- Signal signatures: two isolated muons with opposite charge
- BDT-based categorization to enhance signal sensitivity
  - ➢ Driven by the different Higgs boson production modes
- Data driven approach used for background estimation
- Signal+Background PDF used to fit the observed $m_{\mu\mu}$ spectra simultaneously in all the categories to derive the final signal strength μ (σ_{obs}/σ_{SM})
  - ➢ Signal and background modeled by analytic functions

Event Selection for H→μμ

- Single muon trigger with p_T threshold of 26 or 50 GeV

	Selection
Common preselection	Primary vertex Two opposite-charge muons Muons: $\lvert\eta\rvert < 2.7$, $p_T^{lead} > 27$ GeV, $p_T^{sublead} > 15$ GeV (except VH 3-lepton)
Fit Region	$110 < m_{\mu\mu} < 160$ GeV
Jets	$p_T > 25$ GeV and $\lvert\eta\rvert < 2.4$ or with $p_T > 30$ GeV and $2.4 < \lvert\eta\rvert < 4.5$
$t\bar{t}H$ Category	at least one additional e or μ with $p_T > 15$ GeV, at least one b-jet (85% WP)
VH 3-lepton Categories	$p_T^{sublead} > 10$ GeV, one additional e (μ) with $p_T > 15(10)$ GeV, no b-jets (85% WP)
VH 4-lepton Category	at least two additional e or μ with $p_T > 8, 6$ GeV, no b-jets (85% WP)
ggF +VBF Categories	no additional μ, no b-jets (60% WP)

Selected events sorted into 20 categories in total, which are mutually exclusive and in the order of ttH(1) →VH(3)→VBF(4)→ggF(12)

ttH Categorization

- Target semi/dileptonic decays of the top pair
  - ➢ Requiring ≥1 extra e/μ and ≥1 b-tagged jet
  - ➢ Two highest-p_T muons with opposite charge as the Higgs candidate
- BDT trained to distinguish ttH signal from all backgrounds (ttbar, ttZ, diboson, etc)
  - ➢ Training variables: p_T of e/μ, invariant masses of leptons/tops, as well as jet and b-jet multiplicities, and H_T

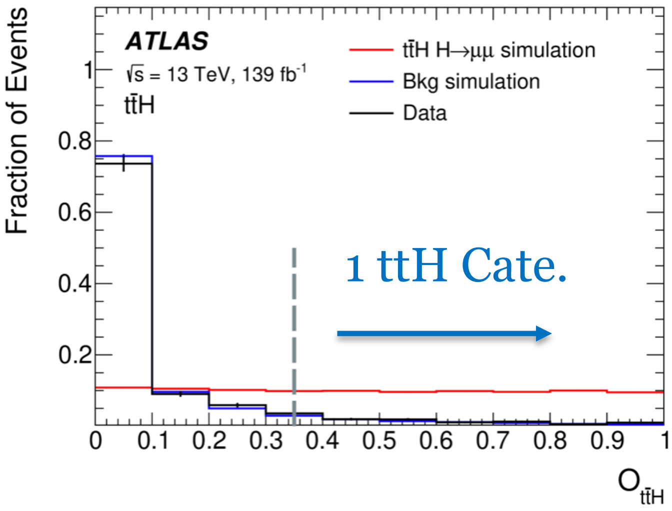

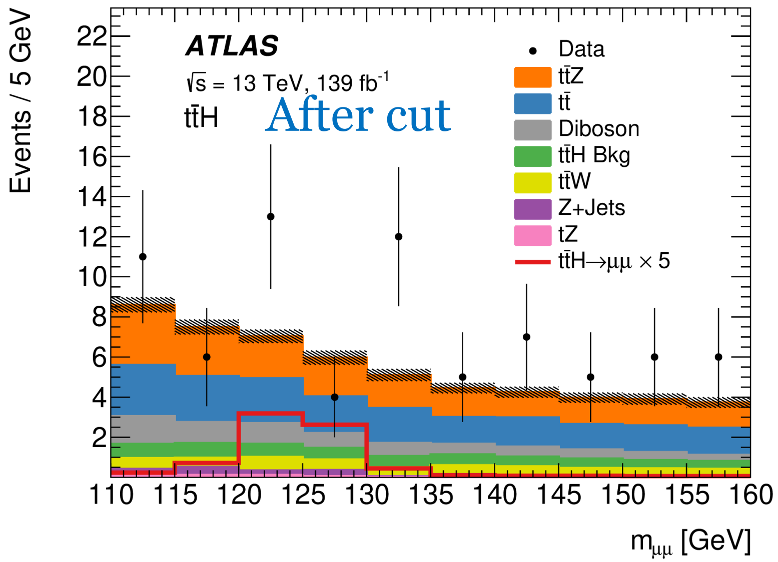

VH Categorization

- Target WH/ZH in leptonic decays: requiring 1/2 additional leptons apart from the dimuon pair
- Two BDTs trained for 3-lepton and 4-lepton cases using invariant mass and angular variables of lepton systems as well as E_T^{miss} and jet multiplicity

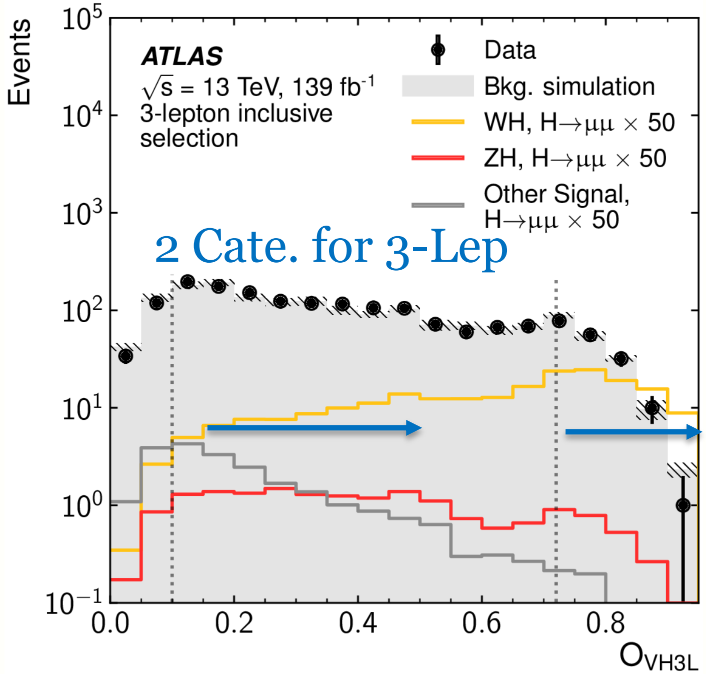

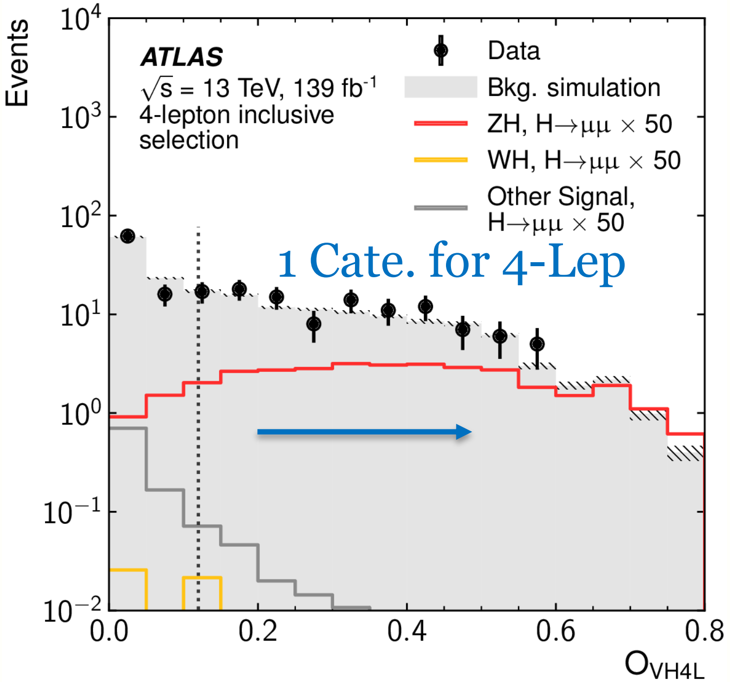

VBF/ggF Categorization (1)

- Events not selected into ttH or VH are classified into 0-jet, 1-jet and ≥2-jet regions
  - Veto events with any b-tagged jet or extra muon
- In the 2-jet region, first a BDT trained to disentangle VBF signal and background: 4 VBF categories defined
- 3 BDTs (ggF&VBF signals against bkg.) trained in each jet-multiplicity region to categorize the remaining events: 4 ggF categories defined based on each BDT
- Training variables: $p_T^{\mu\mu}$, $y_{\mu\mu}$, $\cos\theta^*$, p_T and η of jets, p_T^{jj}, y_{jj}, $\Delta\phi_{jj,\mu\mu}$, m_{jj}, etc

VBF/ggF Categorization (2)

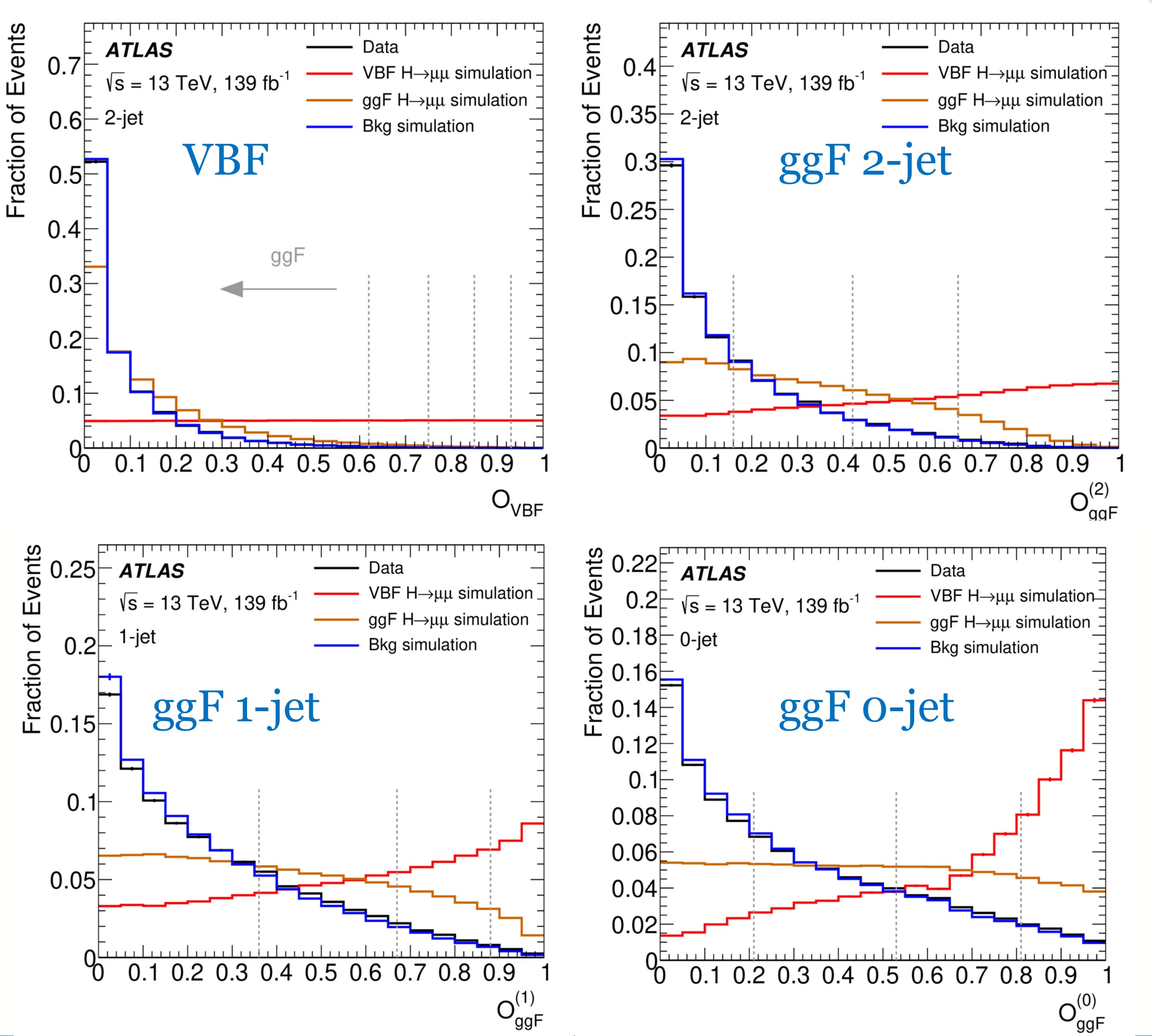

- There are four groups of categories: VBF, ggF-2jet, ggF-1jet and ggF-0jet
- In each group, four categories are defined based on the signal purity

Signal Model

- Signal shape dominated by detector resolution
- Double-sided Crystal Ball function used to model signal
  - ➢ Gaussian core and power-law tails on both sides
- MC spectra created by summing over all production modes in each category
  - ➢ Relative normalization from SM assumed, negligible differences observed between modes

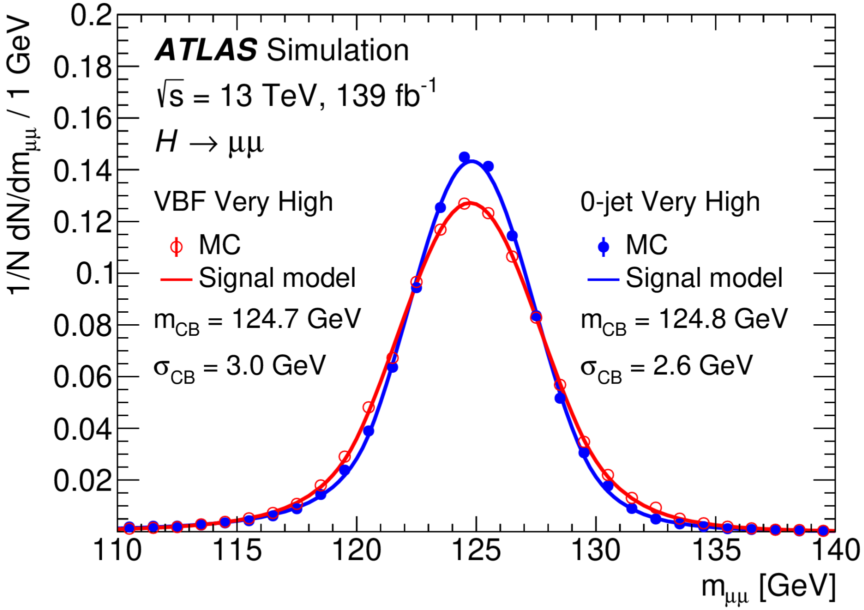

The signal fitting is performed for each category
Crystal Ball width ranges from 2.6 to 3.2 GeV

Background Model

- A "core function" multiplied by an "empirical function" is used to model bkg. shape
  - Core function: a leading-order Drell-Yan line-shape convoluted with a Gaussian function mimicking detector resolution effects
  - Empirical function: used to correct for distortions of the mass shape and smaller background, either a Power law or Epoly function

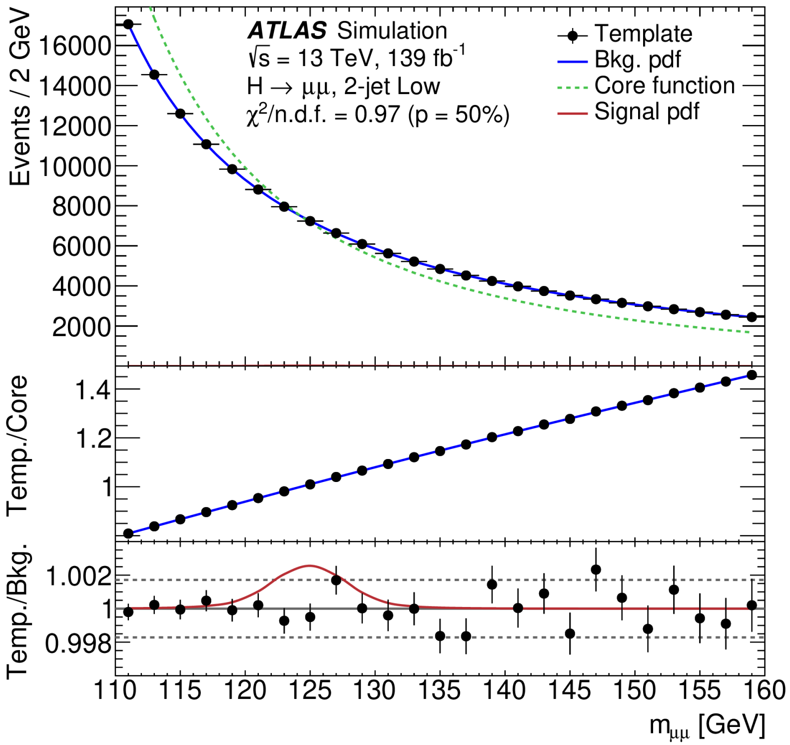

Potential background mis-modeling considered as systematic uncertainty ("spurious signal" referred SS)

H→μμ Results

- A simultaneous maximum-likelihood fit performed to the observed $m_{\mu\mu}$ spectra of in 20 categories
- The measured signal strength is:

$$\textbf{Combined } \mu = 1.17 \pm 0.58(\textit{Stat.})\,{}^{+0.18}_{-0.13}(\textit{sys.})$$

$$= 1.17 \pm 0.58(\textit{Stat.})\,{}^{+0.13}_{-0.08}(\textit{theo.}) \pm 0.10(\textit{SS})\,{}^{+0.07}_{-0.03}(\textit{exp.})$$

- Results are statistical uncertainty dominated
- The observed (expected) significance is 2.0 (1.7)σ

Two papers during Run 2: Phys. Rev. Lett. 119 (2017) 051802 (Editors' suggestion) and Phys. Lett. B 812 (2021) 135980

Reported by CERN Press Release

CERN ABOUT NEWS

News › Press release › Topic: Physics

Voir en français

CERN experiments announce first indications of a rare Higgs boson process

The ATLAS and CMS experiments at CERN have announced new results which show that the Higgs boson decays into two muons

3 AUGUST, 2020

HH → *bb* $\tau\tau$ *and HH Combination*

HH Production

- SM non-resonant HH: $\sigma_{HH}^{ggF} = 31.05$ fb, $\sigma_{HH}^{VBF} = 1.73$ fb
  - ➢ Direct access to Higgs self-coupling and potential

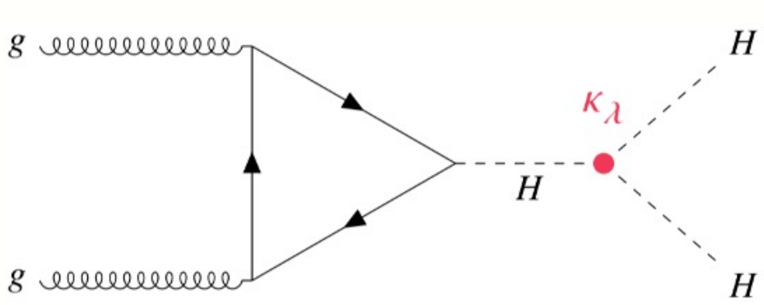

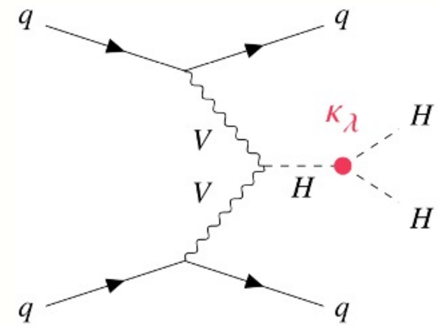

- Various BSM theories predict heavy resonances decaying into HH
  - ➢ Narrow width approximation
  - ➢ 2HDM as benchmark model

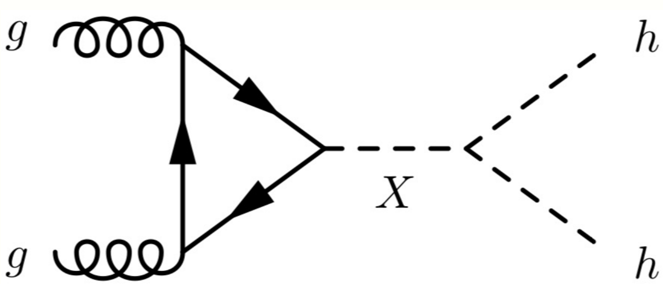

bb$\tau\tau$ Final State

HH Branching Ratios

	bb	WW	ττ	ZZ	γγ
bb	33%				
WW	25%	4.6%			
ττ	7.4%	2.5%	0.39 %		
ZZ	3.1%	1.2%	0.34 %	0.076 %	
γγ	0.26 %	0.10 %	0.029 %	0.013 %	0.005 3%

Di-τ Branching Ratios

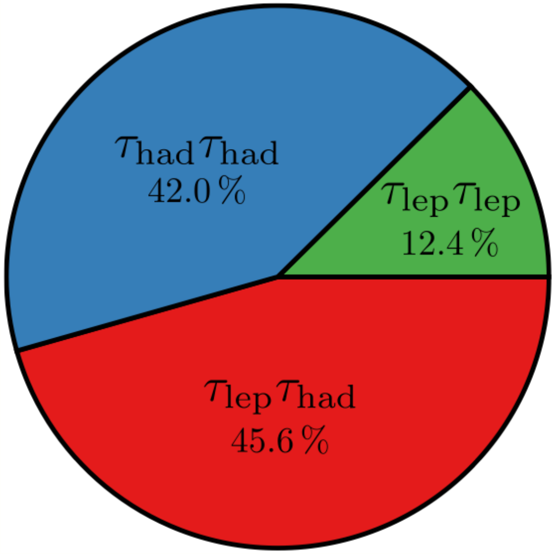

- bb$\tau\tau$: 7.4%, 3rd largest BR, relatively clean signature compared to other channels with higher BR
- Performed in two channels depending on τ decay: $\tau_{had}\tau_{had}$ (42%) and $\tau_{had}\tau_{had}$ (45.6%)

Event Selection

- Signal signature: two b-jets (DNN-based tagger, 77%) and $\tau_{\text{had}}\tau_{\text{had}}/\tau_{\text{lep}}\tau_{\text{had}}$ with opposite charge

Signal region	Tau/Lepton	Trigger
$\tau_{\text{had}}\tau_{\text{had}}$	2 hadronic τ	Single or Di-tau Trigger (STT/DTT)
$\tau_{\text{lep}}\tau_{\text{had}}$ SLT	1 hadronic τ + 1 e/μ	Single lepton trigger (SLT)
$\tau_{\text{lep}}\tau_{\text{had}}$ LTT	1 hadronic τ + 1 e/μ	Lepton+tau trigger (LTT)

- Trigger-dependent thresholds on e/μ/τ_{had} and jets
- e/μ veto applied for $\tau_{\text{had}}\tau_{\text{had}}$; exactly 1 e/μ for $\tau_{\text{lep}}\tau_{\text{had}}$
- $m_{\tau\tau}^{MMC}$ > 60 GeV for all channels; m_{bb} < 150 GeV applied for $\tau_{\text{lep}}\tau_{\text{had}}$

Background Estimation

- ttbar with true τ_{had}: shape from simulation, normalization determined in the fit
- Z + heavy-flavor: shape from simulation, normalization from a dedicated Z(→ll)+heavy-flavor control region in the fit
- Single Higgs and other processes: estimated from simulation
- Jets → fake τ_{had} background: estimated with data-driven approach (shown in next three slides)

Fake τ_{had} Background in $\tau_{lep}\tau_{had}$

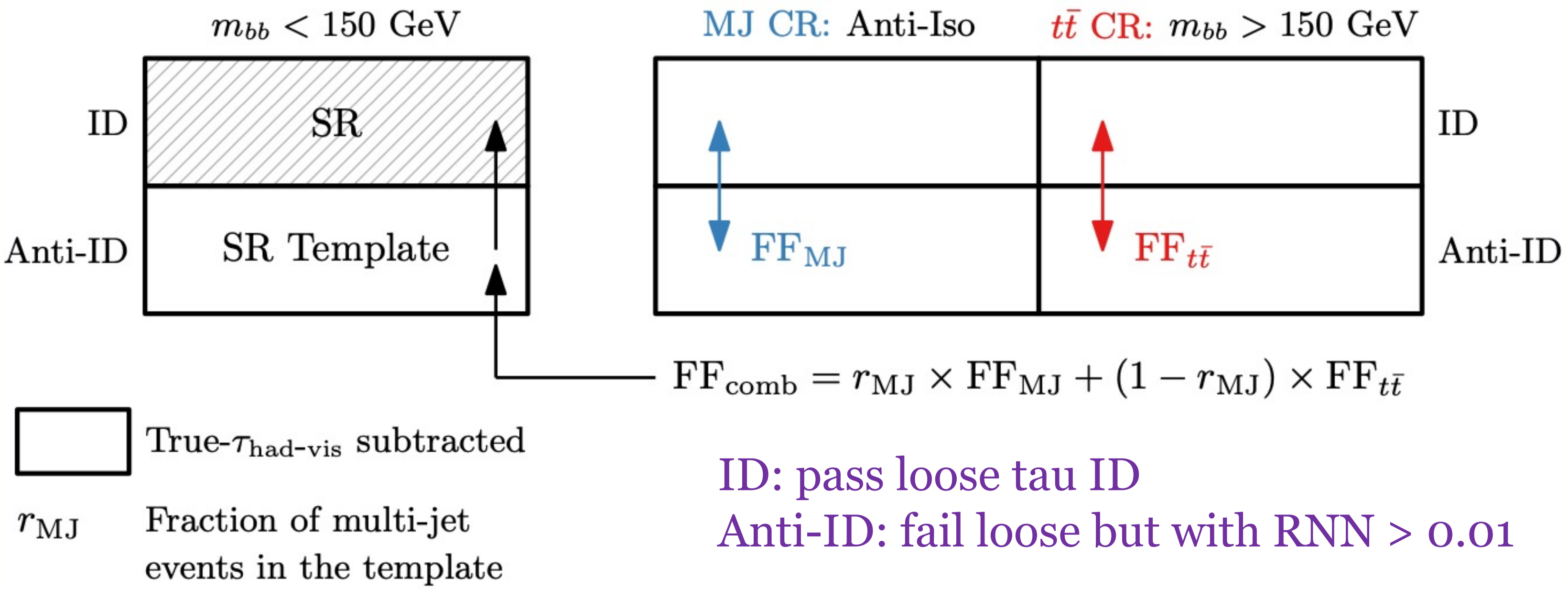

ID: pass loose tau ID
Anti-ID: fail loose but with RNN > 0.01

- Fake factor (FF) derived for ttbar and multi-jet separately
  - Split in 1/3-prong and derived as a function of τ_{had} p_T
- Combined FFs applied to scale Anti-ID SR template to obtain fake τ_{had} background in SR

Fake τ_{had} Background in $\tau_{had}\tau_{had}$

- Different methods used for ttbar and multi-jet
  - multi-jet: both τ_{had} are fake, FF method used
  - ttbar: predominantly only one reconstructed is τ_{had} fake, scale-factors method used

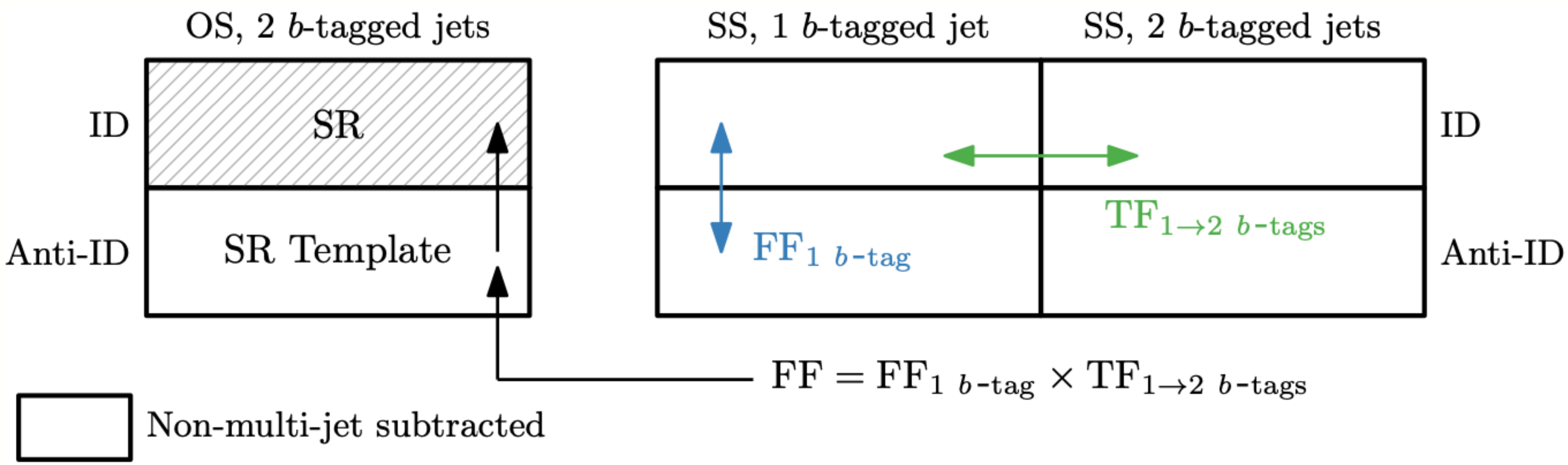

For multi-jet, FF derived in 1 b-tag same-sign CR
Transfer factors (TFs) derived to account for extrapolation from 1 b-tag to 2 b-tag events

Fake τ_{had} Background in $\tau_{had}\tau_{had}$

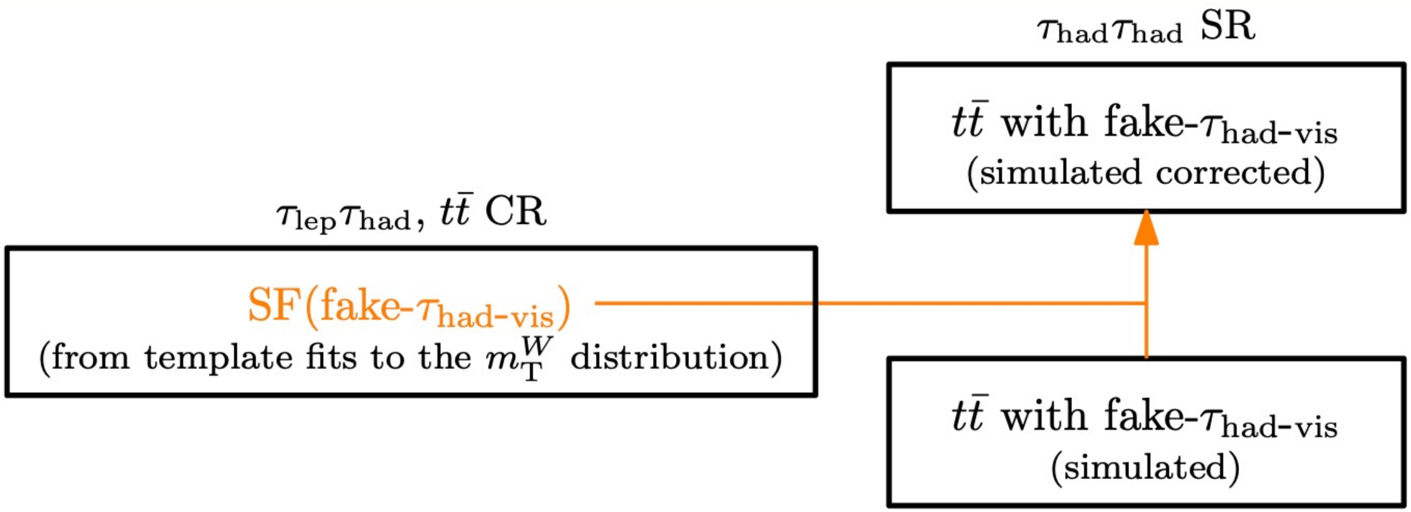

- Fake τ_{had} from ttbar estimated using simulation
- Scale Factor (SF): used to correct τ_{had} misidentification efficiencies; determined by fitting the m_T^W distribution of MC to data in ttbar CR from $\tau_{lep}\tau_{had}$ SLT category
  - ➢ 1 prong: close to 1 below 40 GeV, ~0.6 above 70 GeV
  - ➢ 3 prong: ~20% larger than the 1 prong SFs

Non-resonant Signal Extraction

- MVA trained to separate SM signal and total background
  - $\tau_{had}\tau_{had}$: BDT; $\tau_{lep}\tau_{had}$: neural network
  - Input variables: m_{HH}, m_{bb}, $m_{\tau\tau}^{MMC}$, $\Delta R(b,b)$, $\Delta R(\tau,\tau)$, E_T^{miss}, $\Delta\phi(l\tau,bb)$...etc
  - Output scores used as final discriminant

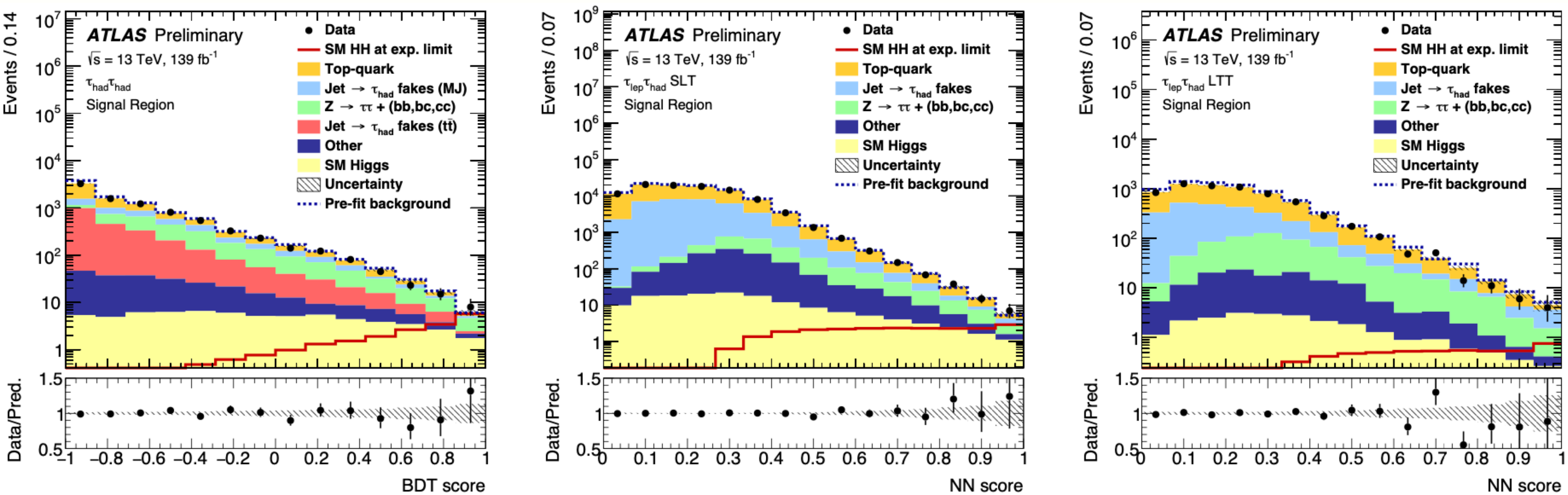

Resonant Signal Extraction

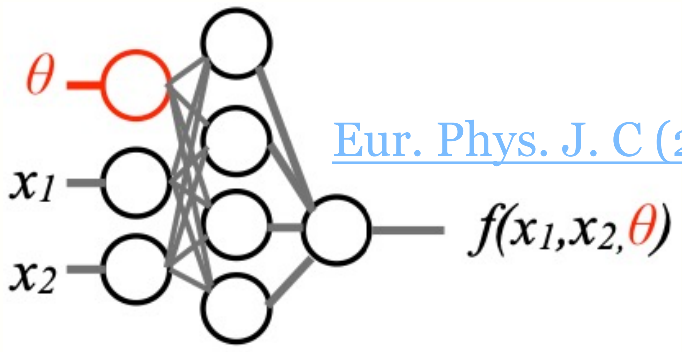

Eur. Phys. J. C (2016) 76:235

- Parametrized neural networks (PNN) used as discriminant
  - ➢ Parametrized in mass of scalar ($\theta = m_X$)
  - ➢ Training variables same as non-resonant case
- Single classifier (per channel) for all considered m_X

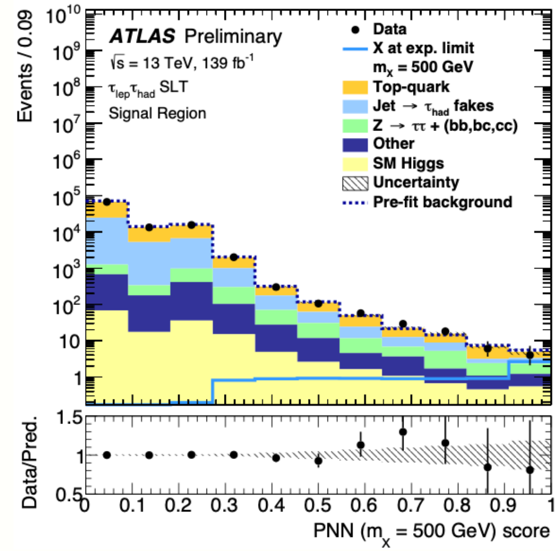

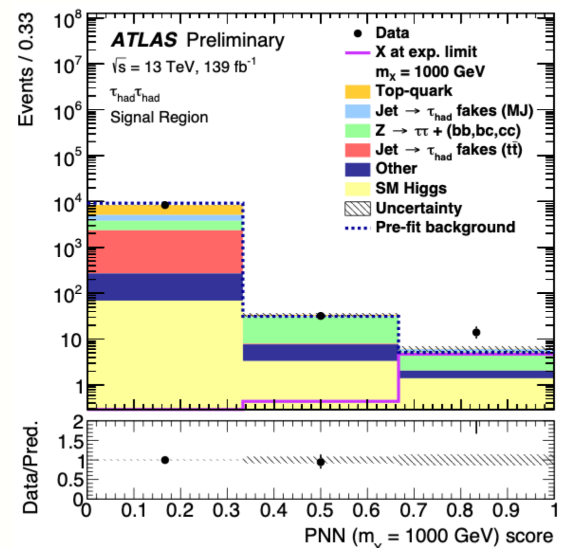

Uncertainties

Uncertainty source	Non-resonant HH
Data statistical	81%
Systematic	59%
$t\bar{t}$ and Z + HF normalisations	4%
MC statistical	28%
Experimental	
Jet and E_{T}^{miss}	7%
b-jet tagging	3%
$\tau_{had\text{-}vis}$	5%
Electrons and muons	2%
Luminosity and pileup	3%
Theoretical and modelling	
Fake-$\tau_{had\text{-}vis}$	9%
Top-quark	24%
$Z(\rightarrow \tau\tau)$ + HF	9%
Single Higgs boson	29%
Other backgrounds	3%
Signal	5%

- Breakdown of the relative contributions to the unc. in the extracted signal XS
- Data statistic unc. dominated for now
- Leading sys. sources:
  - MC statistical unc.
  - Theory unc. on top and single Higgs processes

Resonant HH→bbττ Results

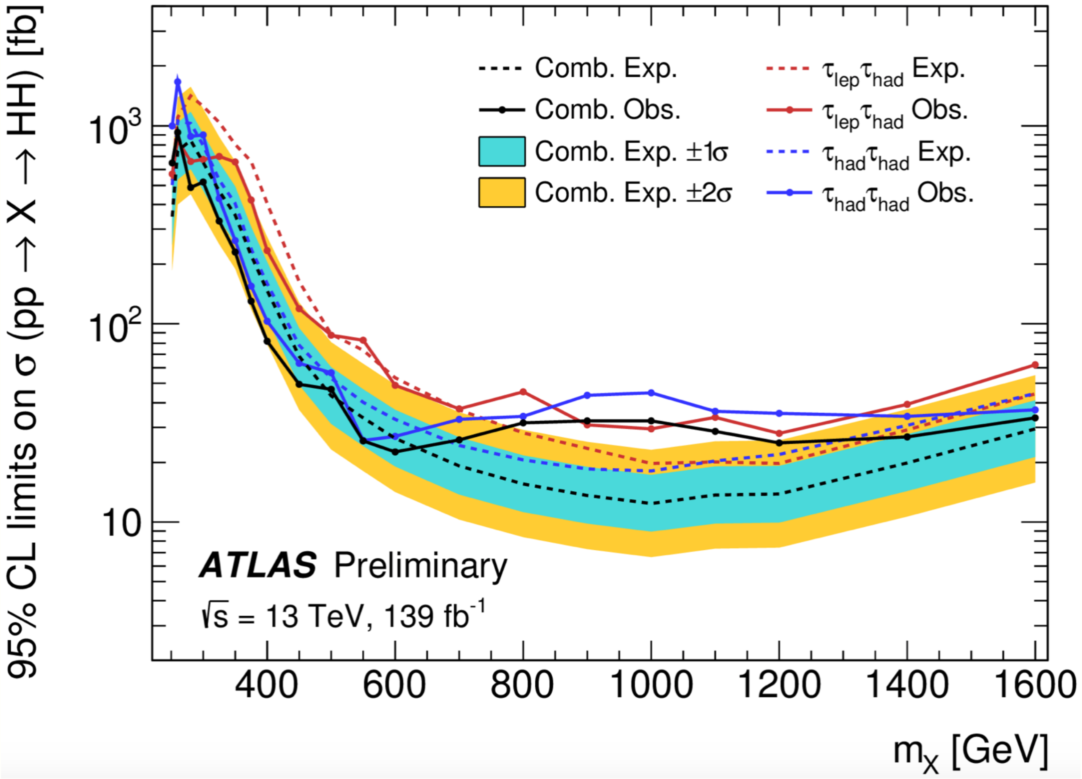

Observed (expected) upper limits: 920-23 fb (840-12 fb) depending on the mass region
Local (global) significance for 1 TeV is 3.0σ (2.0σ)

Results

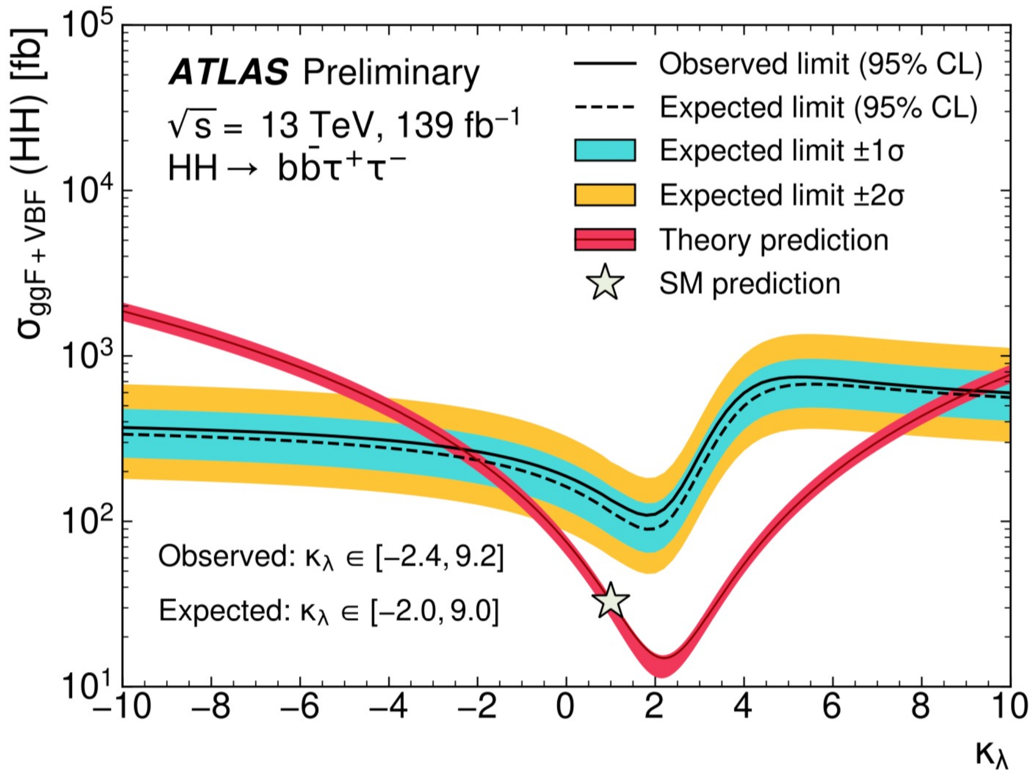

ATLAS-CONF-2021-030
ATLAS-CONF-2021-052

Observed (expected) limit at 95% CL: 4.7 (3.9) × σ_{SM}
4x improvement over 36.1 fb^{-1} result (12.7 × σ_{SM})

Observed (expected) constraint on κ_λ: $-2.4 \le \kappa_\lambda \le 9.2$ ($-2.0 \le \kappa_\lambda \le 9.0$)

HH Combination

- Performed statistical combination for different HH analyses to maximize sensitivity to HH production
- Resonant: including $bb\tau\tau$, $bb\gamma\gamma$ and bbbb
- Non-resonant: including $bb\tau\tau$ and $bb\gamma\gamma$
  - $bb\tau\tau$ outperforms at around $\kappa_\lambda = 1$ due to more boosted signal and higher BR, while $bb\gamma\gamma$ outperforms at high κ_λ values due to high acceptance
- Systematics correlated where appropriate (like luminosity, flavor tagging, signal theory uncertainties, etc)

Resonant Combination Result

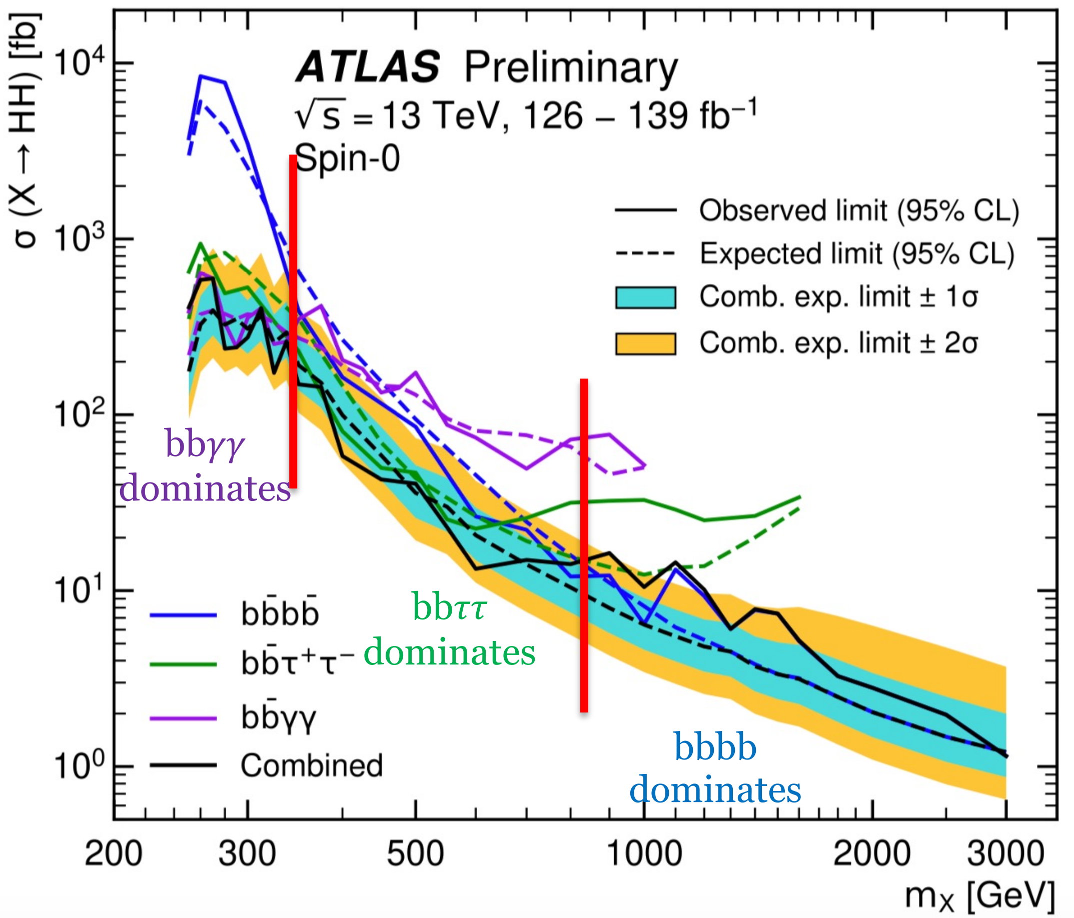

No statistically significant excess found, largest excess at 1.1 TeV: local (global) significance is 3.2σ (2.1σ)

Non-resonant Combination Result

ATLAS-CONF-2021-052

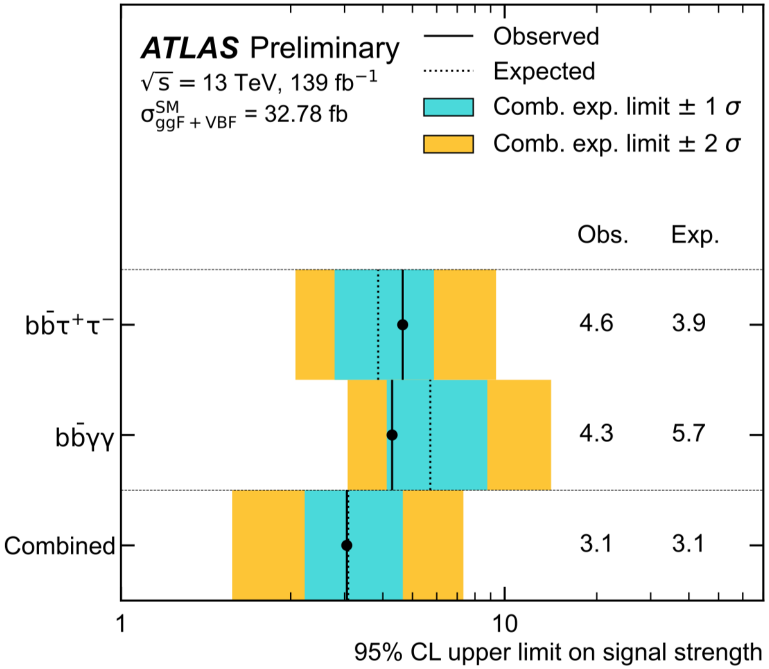

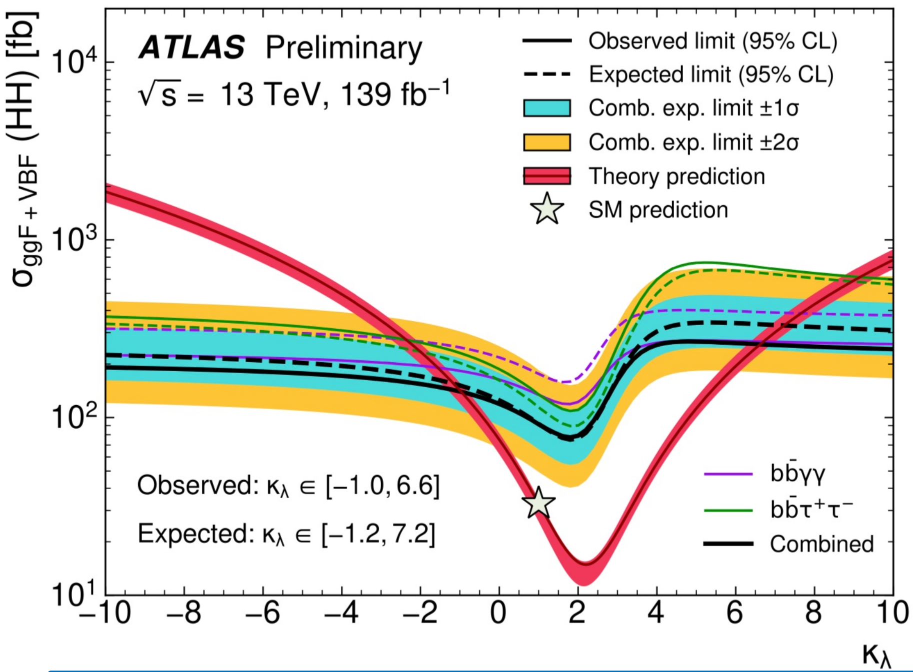

Obs. (exp.) limits: 3.1 (3.1) × σ_{SM}

Obs. (exp.) constraint on κ_λ: -1.0 ≤ κ_λ ≤ 6.6 (-1.2 ≤ κ_λ ≤ 7.2)

The best constraints on HH signal strength and κ_λ to date!

Reported by CERN Courier

CERNCOURIER | Reporting on international high-energy physics

Physics ▾ | Technology ▾ | Community ▾ | In focus | Magazine

HIGGS AND ELECTROWEAK | NEWS

Extending the reach on Higgs' self-coupling

11 March 2022

HH+H combination aiming for Higgs Symposium: expected to provide the most sensitive results on κ_{λ} and κ_{2V} (VVHH coupling)

Summary

- Presented the Yukawa couplings and self-coupling studies based on the Run 2 dataset
- The measurements are in line with the SM prediction, and the most stringent results achieved at ATLAS
- The LHC Run 3 will provide more room for exploring the Yukawa couplings and HH processes
  - Possible evidence for $H\rightarrow\mu\mu$ at ATLAS, observation combining ATLAS and CMS analyses

Backup

Particle Identifications at ATLAS

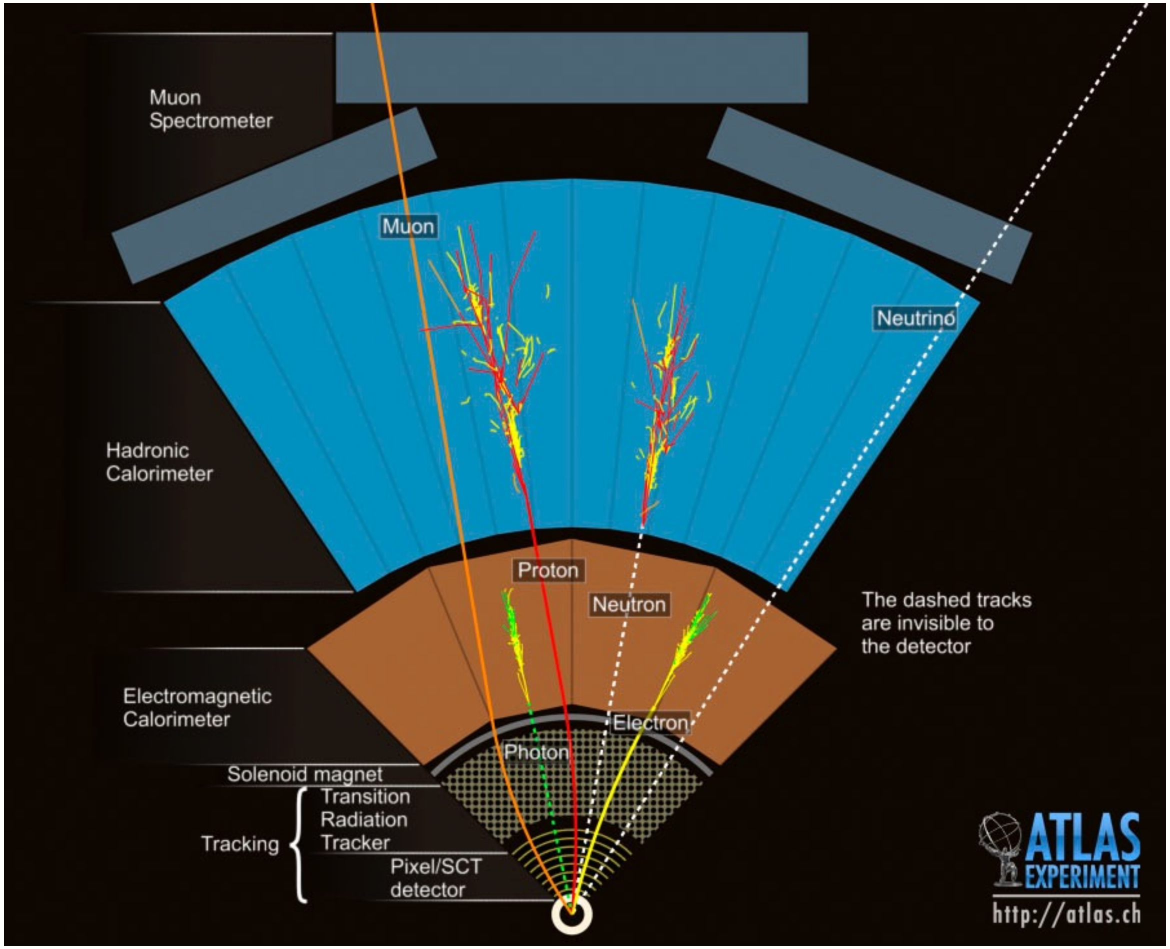

The main final-state particles used for the physics analysis: electron, muon, tau, jet, b-jet, and missing transverse energy E_T^{miss}

Different types of particles interact with certain sensitive sub-detectors and give different responses in the experiments

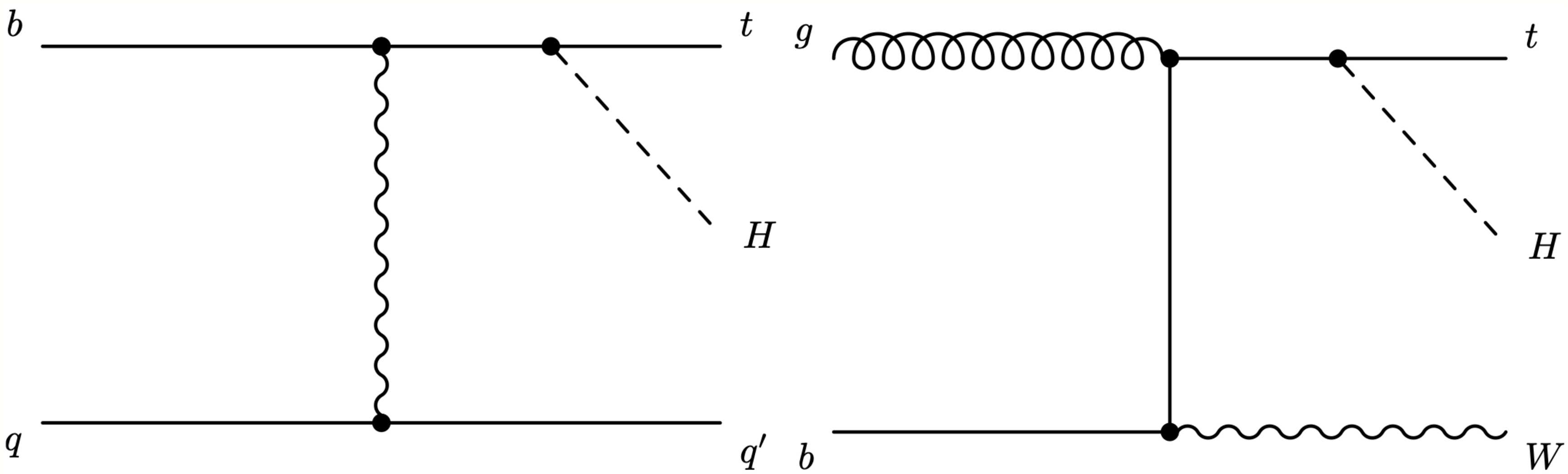
b
t
H
q
q'
g
t
H
b
W

[JHEP 04 (2014) 004]

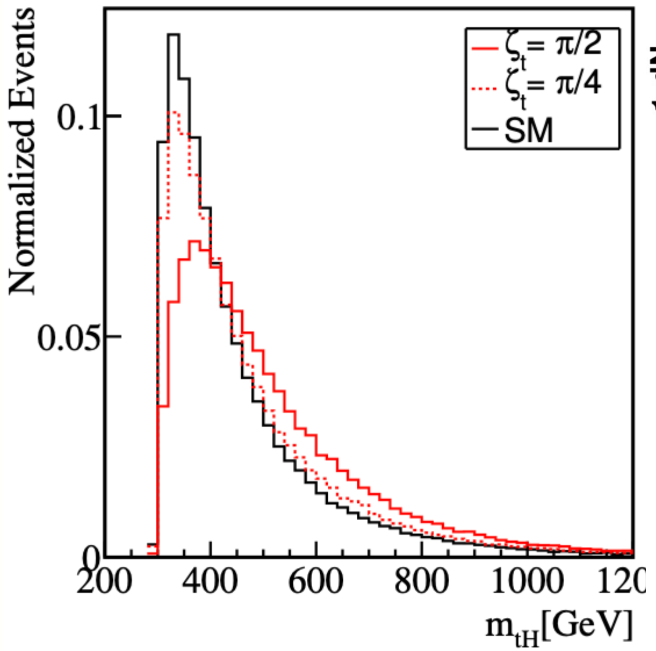

[Phys. Rev. D 92, 015019]

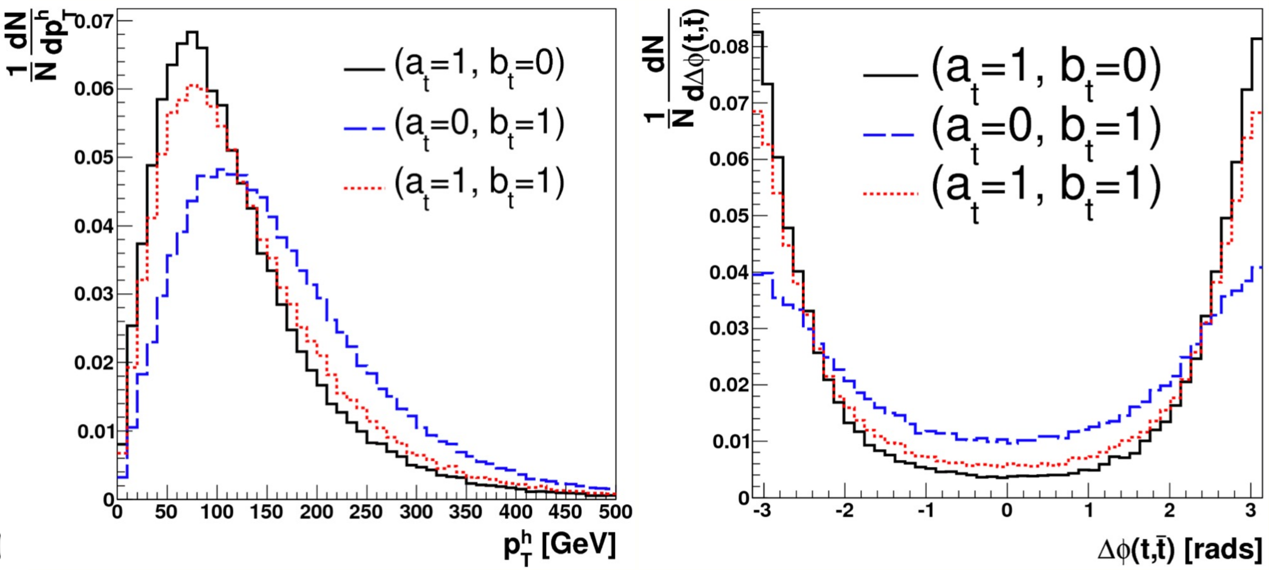

Fitting Procedure

- A simultaneous maximum-likelihood fit is performed to the observed $m_{\gamma\gamma}$ spectra in all the categories
- The likelihood model is parameterized into κ_t and α, which are the parameters of interest in the fit
- The parameters of the background model and background normalization in each category are left free in the fit
- All the systematic uncertainties are considered as nuisance parameters in the fit

Background Rejection and CP BDTs

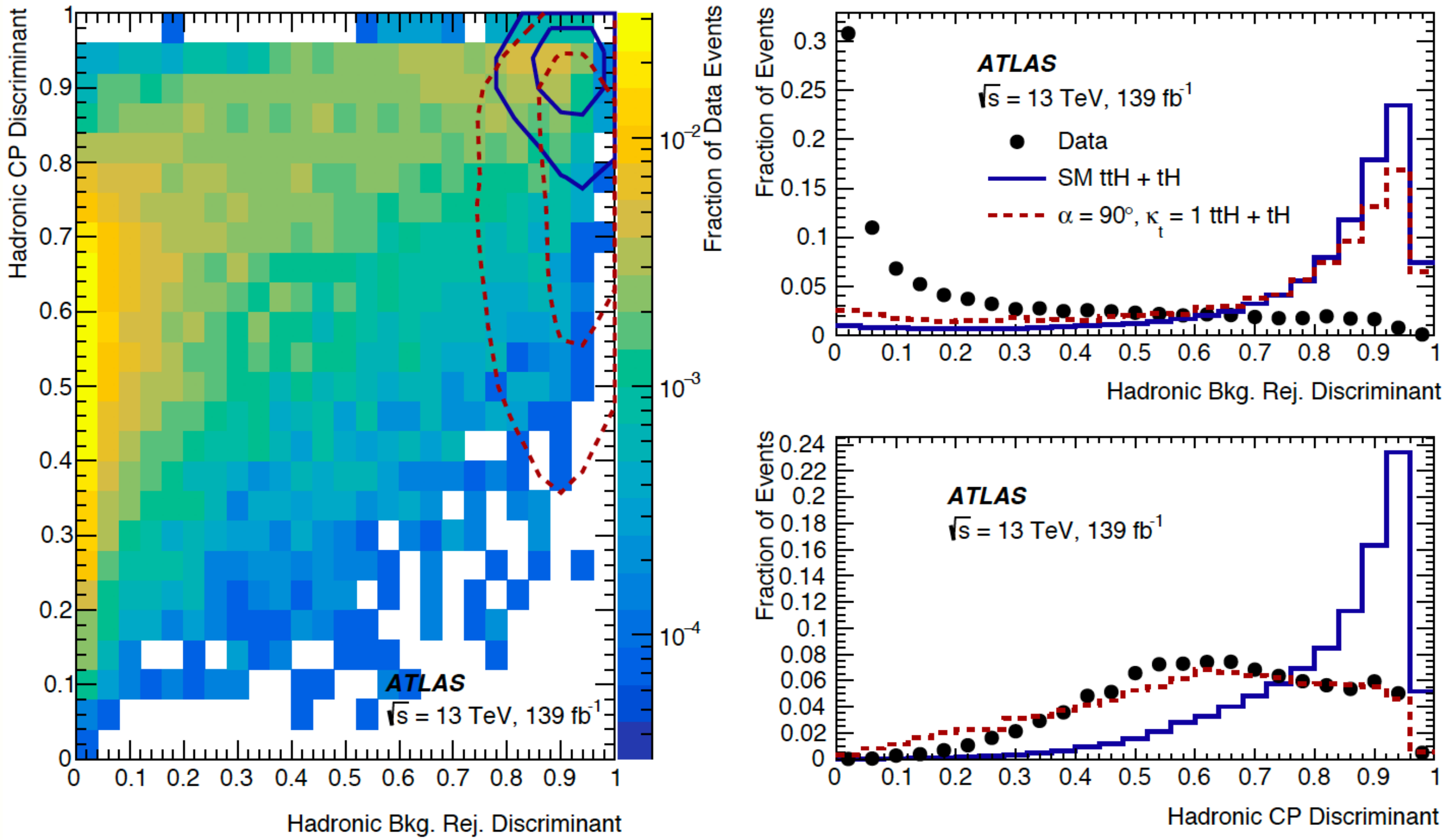

The BDTs from Had region shown here as an example; contours contain 25% and 50% of the events

ttH/tH (H→γγ): Yield Parametrization

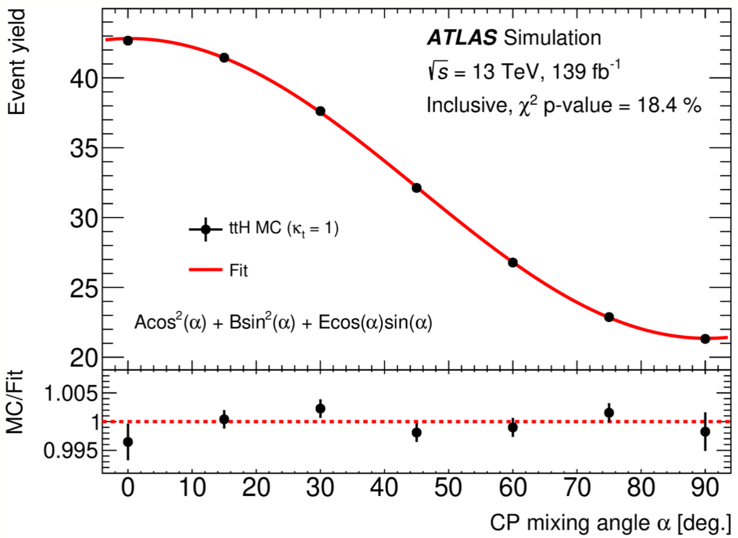

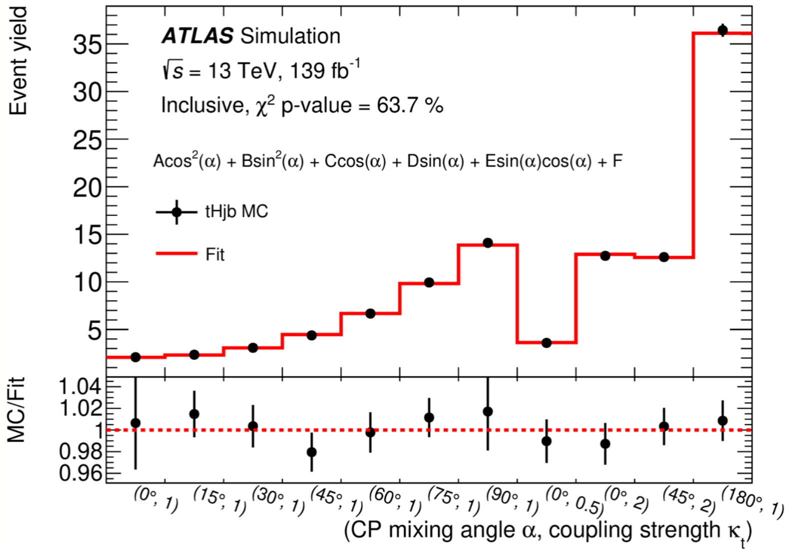

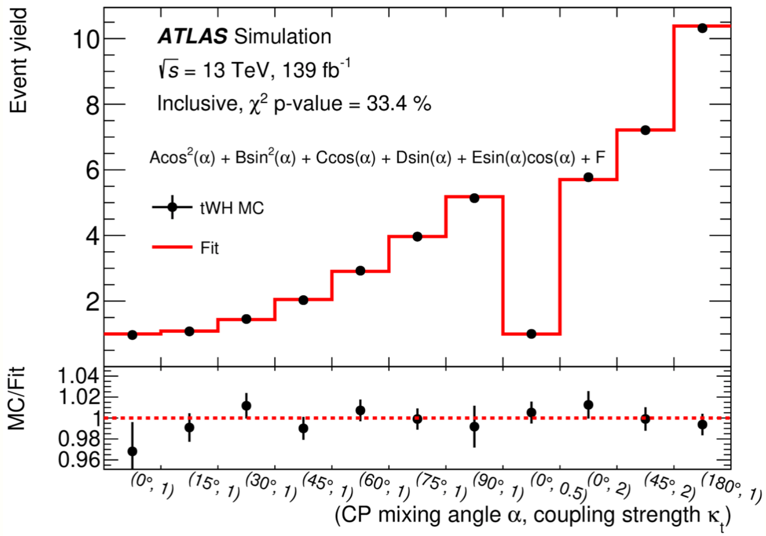

Systematic Uncertainties

- This analysis is dominated by statistical uncertainties of background events. The impact of systematic uncertainties on the results is found to be negligible. The main systematic sources:
  - Parton showering for ttH, tH and ggH (Pythia vs Herwig), < 10% in the most sensitive categories
  - For ggF, VBF and VH, a 100% theoretical uncertainty in the modeling of the radiation of additional heavy-flavor jets applied
  - Experimental uncertainties from luminosity, trigger, lepton, photon, jet, b-tagging and E_T^{miss}
  - Bias from potential background mis-modeling

Inclusive Data Spectra

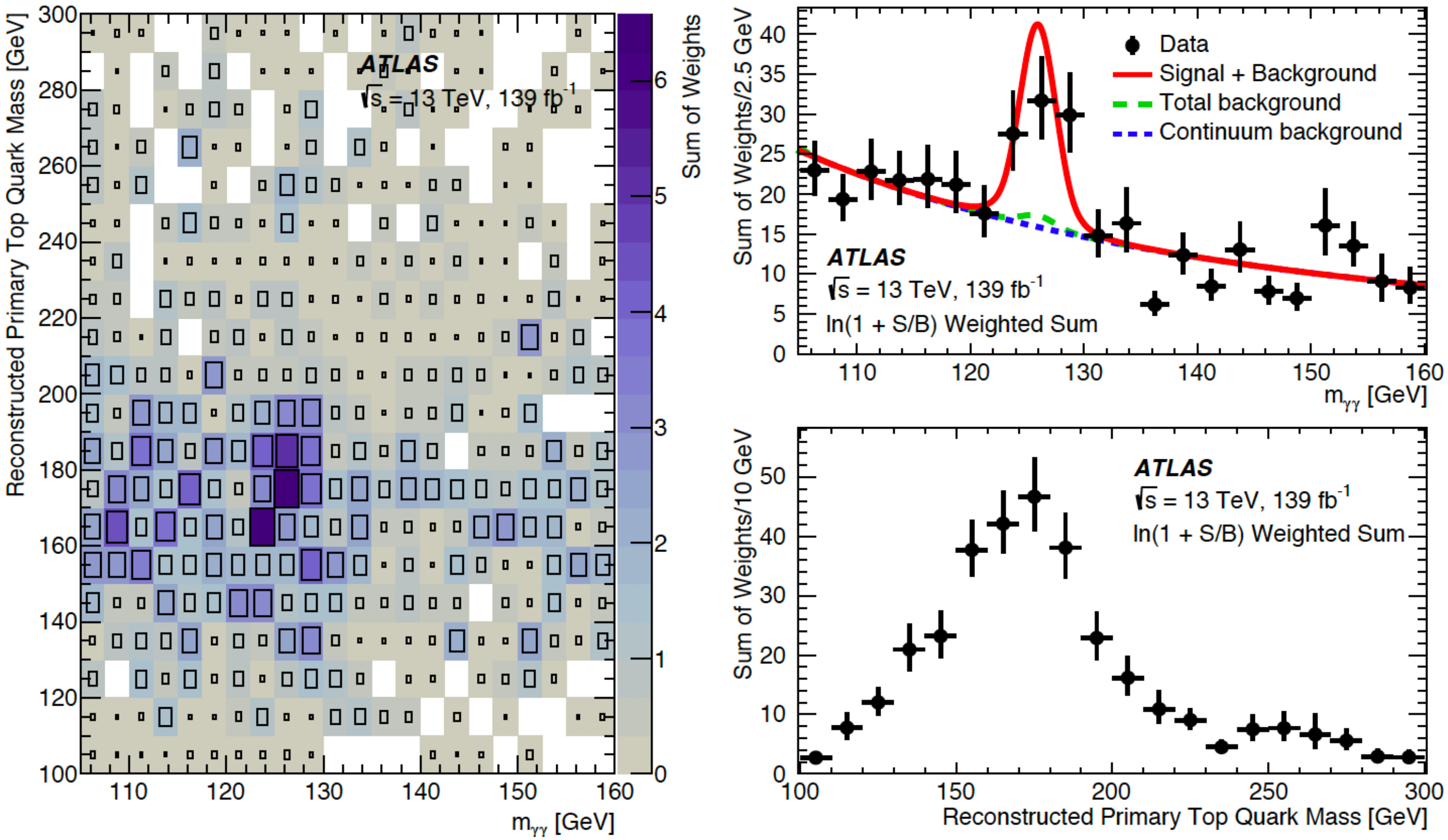

Events and PDFs are weighted by ln(1+S/B) of each category, where S and B are calculated in the smallest $m_{\gamma\gamma}$ interval containing 90% of the signal

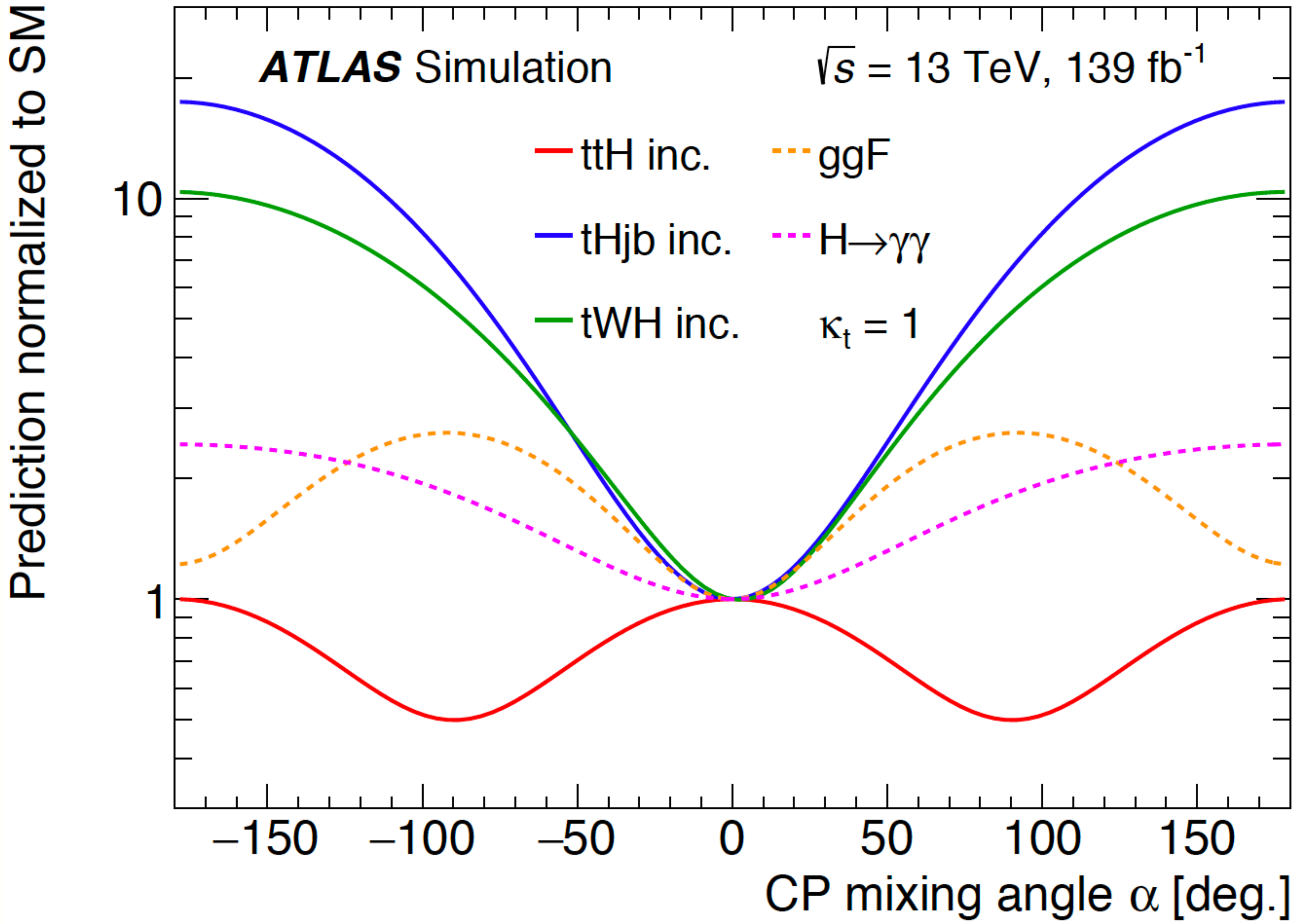
Prediction normalized to SM
ATLAS Simulation
√s = 13 TeV, 139 fb-1
ttH inc.
tHjb inc.
tWH inc.
ggF
H→γγ
κt = 1
10
1
−150
−100
−50
0
50
100
150
CP mixing angle α [deg.]

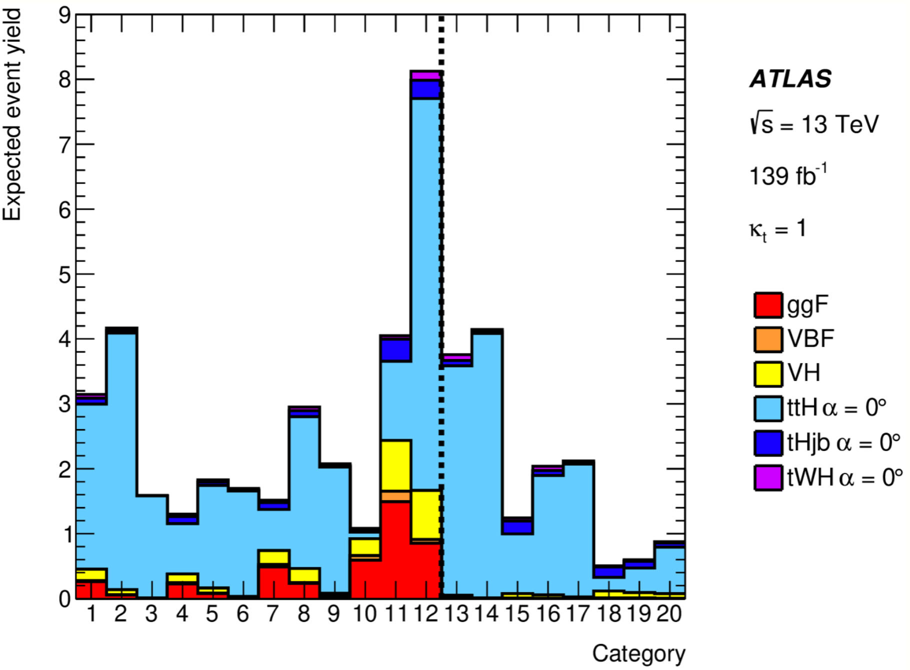
Expected event yield
0
1
2
3
4
5
6
7
8
9
1 2 3 4 5 6 7 8 9 10 11 12 13 14 15 16 17 18 19 20
Category
ATLAS
√s = 13 TeV
139 fb-1
κt = 1
ggF
VBF
VH
ttH α = 0°
tHjb α = 0°
tWH α = 0°

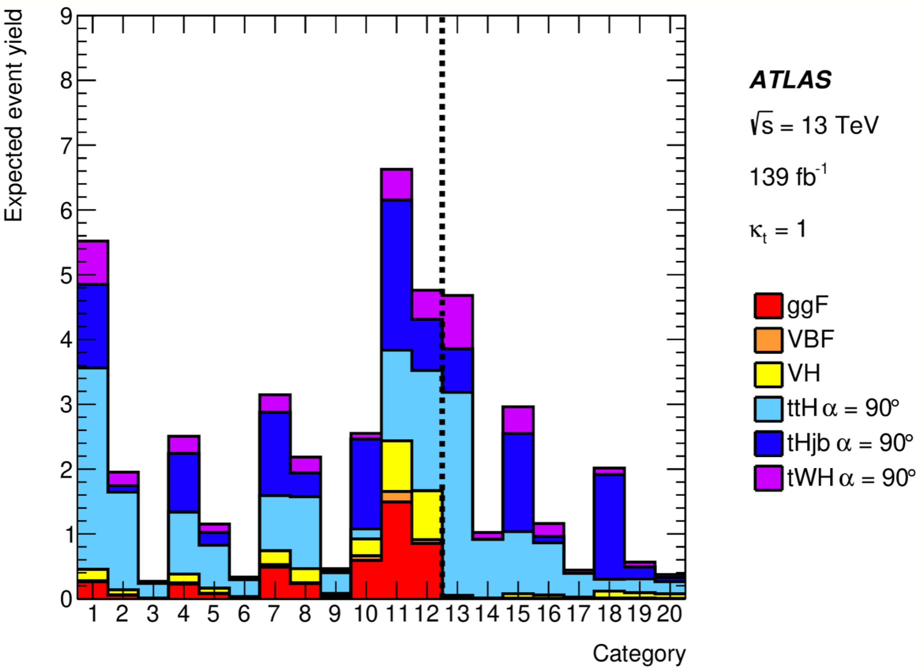
Expected event yield
0
1
2
3
4
5
6
7
8
9
1 2 3 4 5 6 7 8 9 10 11 12 13 14 15 16 17 18 19 20
Category
ATLAS
√s = 13 TeV
139 fb-1
κt = 1
ggF
VBF
VH
ttH α = 90°
tHjb α = 90°
tWH α = 90°

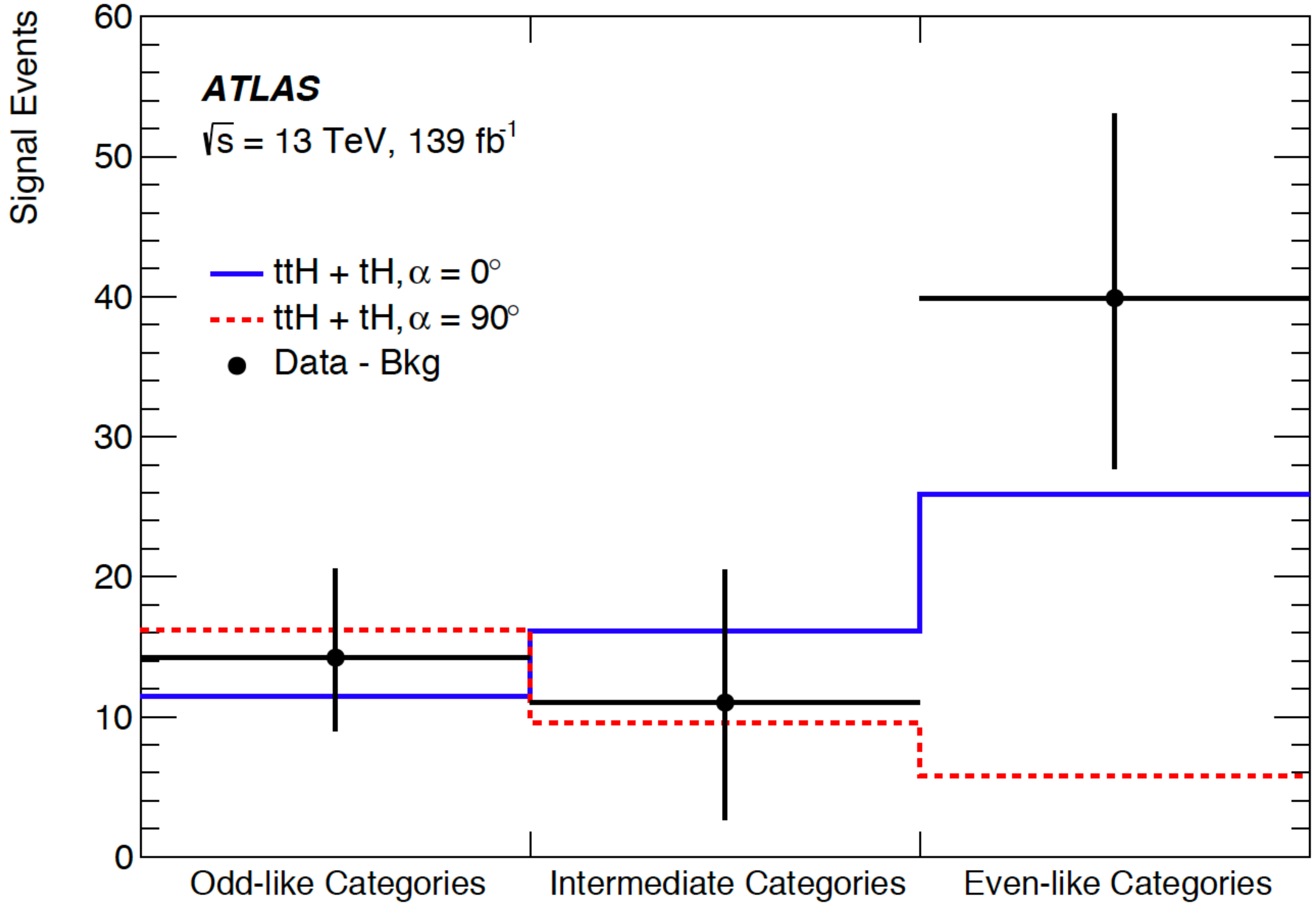
ATLAS
$\sqrt{s}$ = 13 TeV, 139 fb^{-1}
Signal Events
ttH + tH, α = 0°
ttH + tH, α = 90°
Data - Bkg
0
10
20
30
40
50
60
Odd-like Categories
Intermediate Categories
Even-like Categories

Display for a ttH($\rightarrow\gamma\gamma$)-Like Event

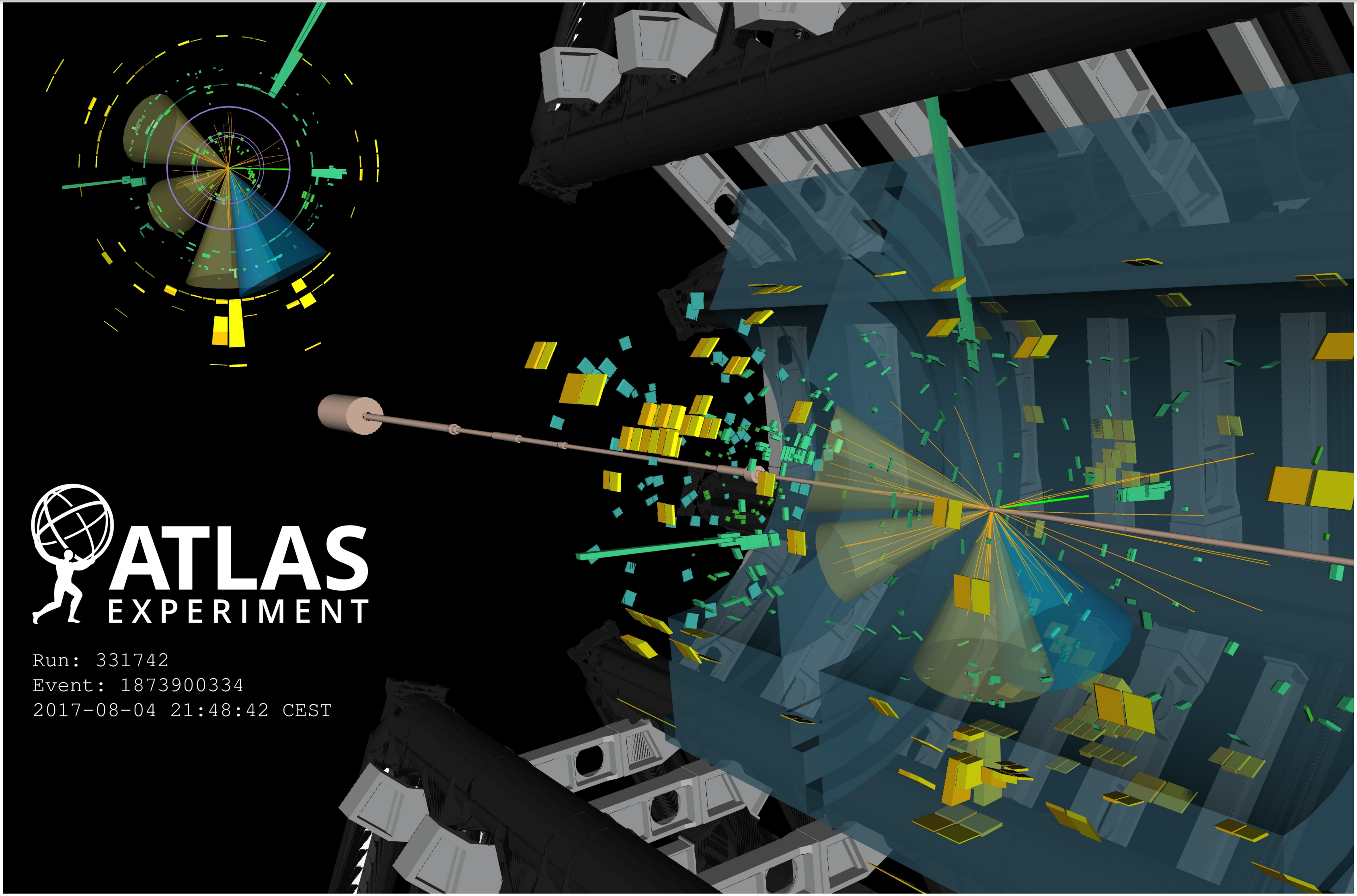

H→μμ: FSR Recovery

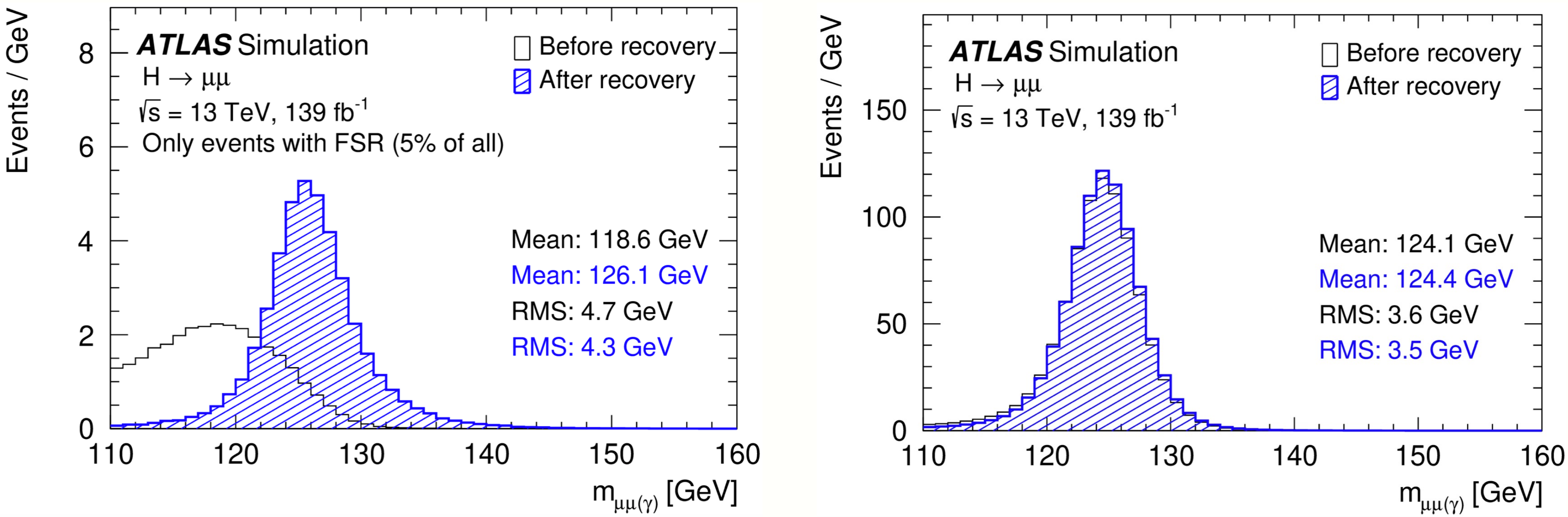

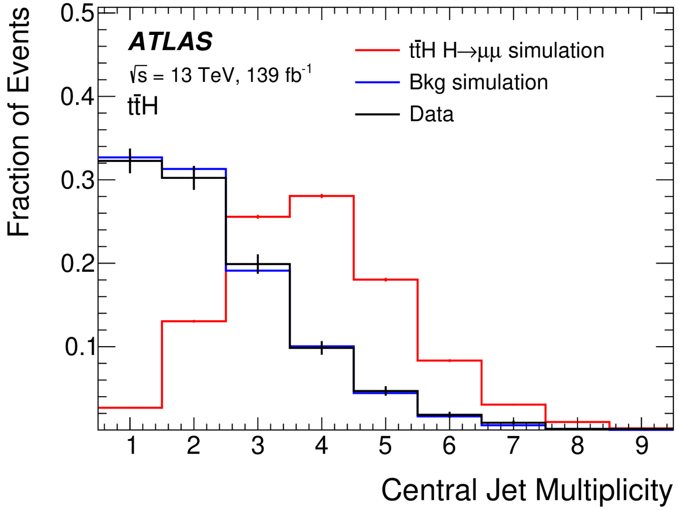

ATLAS
√s = 13 TeV, 139 fb-1
tt̄H
tt̄H H→μμ simulation
Bkg simulation
Data
Fraction of Events
Central Jet Multiplicity

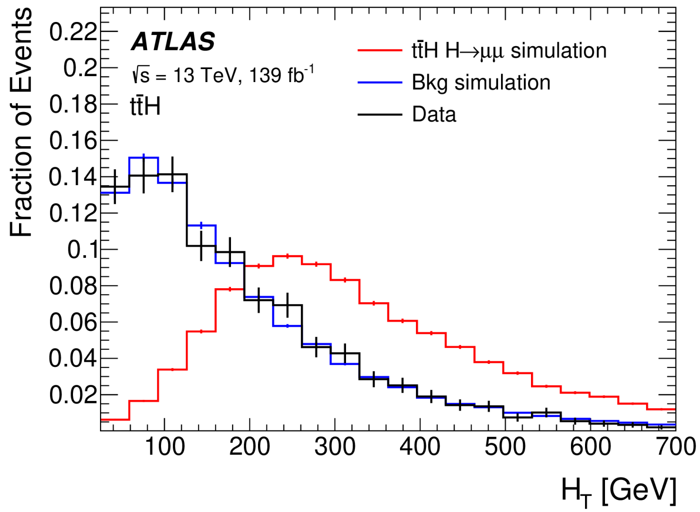

ATLAS
√s = 13 TeV, 139 fb-1
tt̄H
tt̄H H→μμ simulation
Bkg simulation
Data
Fraction of Events
H_T [GeV]

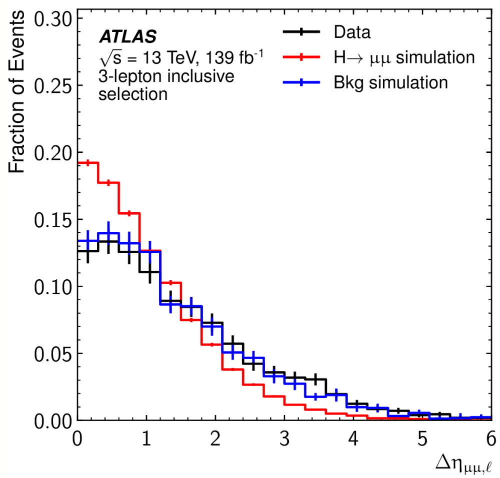

ATLAS
√s = 13 TeV, 139 fb-1
3-lepton inclusive selection
Data
H→ μμ simulation
Bkg simulation
Fraction of Events
Δη_μμ,ℓ

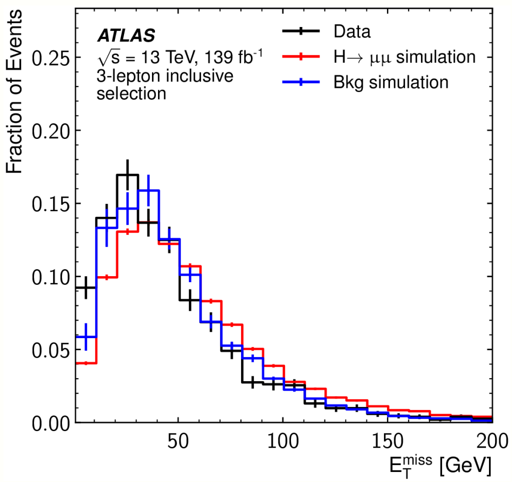

ATLAS
√s = 13 TeV, 139 fb-1
3-lepton inclusive selection
Data
H→ μμ simulation
Bkg simulation
Fraction of Events
E_T^miss [GeV]

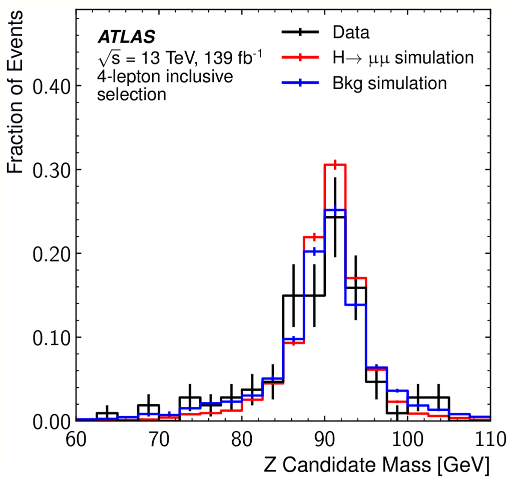

ATLAS
√s = 13 TeV, 139 fb-1
4-lepton inclusive selection
Data
H→ μμ simulation
Bkg simulation
Fraction of Events
Z Candidate Mass [GeV]

VBF/ggF Categorization

- Training variables used:
  - 0-jet: $p_T^{\mu\mu}$, $y_{\mu\mu}$ and $\cos\theta^*$
  - 1-jet: 0-jet variables + p_T^{j1}, η_{j1}, $\Delta\phi_{j1,\mu\mu}$ and $N_{track}^{j_1}$
  - 2-jet: 1-jet + p_T^{j2}, η_{j2}, $\Delta\phi_{j2,\mu\mu}$, p_T^{jj}, y_{jj}, $\Delta\phi_{jj,\mu\mu}$, m_{jj}, E_T^{miss}, H_T and $N_{track}^{j_2}$

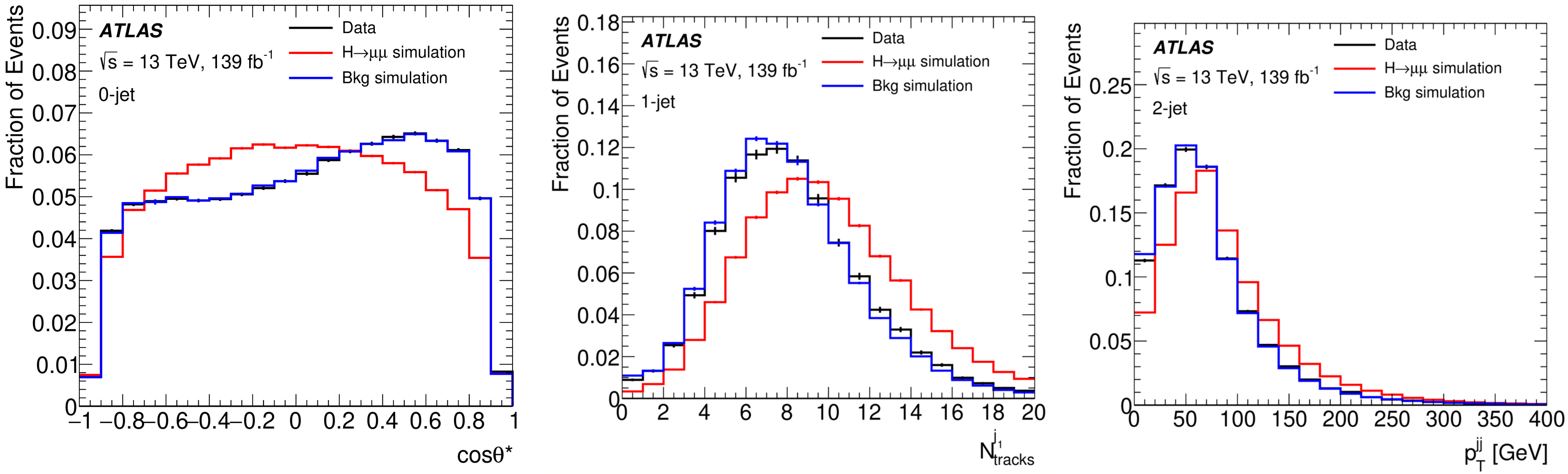

Categorization Performance (1)

Category	Data	S_{SM}	S	B	$S/\sqrt{B}$	S/B [%]	σ [GeV]
VBF Very High	15	2.81 ± 0.27	3.3 ± 1.7	14.5 ± 2.1	0.86	22.6	3.0
VBF High	39	3.46 ± 0.36	4.0 ± 2.1	32.5 ± 2.9	0.71	12.4	3.0
VBF Medium	112	4.8 ± 0.5	5.6 ± 2.8	85 ± 4	0.61	6.6	2.9
VBF Low	284	7.5 ± 0.9	9 ± 4	273 ± 8	0.53	3.2	3.0
2-jet Very High	1030	17.6 ± 3.3	21 ± 10	1024 ± 22	0.63	2.0	3.1
2-jet High	5433	50 ± 8	58 ± 30	5440 ± 50	0.77	1.0	2.9
2-jet Medium	18 311	79 ± 15	90 ± 50	$18\,320 \pm 90$	0.66	0.5	2.9
2-jet Low	36 409	63 ± 17	70 ± 40	$36\,340 \pm 140$	0.37	0.2	2.9
1-jet Very High	1097	16.5 ± 2.4	19 ± 10	1071 ± 22	0.59	1.8	2.9
1-jet High	6413	46 ± 7	54 ± 28	6320 ± 50	0.69	0.9	2.8
1-jet Medium	24 576	90 ± 11	100 ± 50	$24\,290 \pm 100$	0.67	0.4	2.7
1-jet Low	73 459	125 ± 17	150 ± 70	$73\,480 \pm 190$	0.53	0.2	2.8
0-jet Very High	15 986	59 ± 11	70 ± 40	$16\,090 \pm 90$	0.55	0.4	2.6
0-jet High	46 523	99 ± 13	120 ± 60	$46\,190 \pm 150$	0.54	0.3	2.6
0-jet Medium	91 392	119 ± 14	140 ± 70	$91\,310 \pm 210$	0.46	0.2	2.7
0-jet Low	121 354	79 ± 10	90 ± 50	$121\,310 \pm 280$	0.26	0.1	2.7
VH4L	34	0.53 ± 0.05	0.6 ± 0.3	24 ± 4	0.13	2.6	2.9
VH3LH	41	1.45 ± 0.14	1.7 ± 0.9	41 ± 5	0.27	4.2	3.1
VH3LM	358	2.76 ± 0.24	3.2 ± 1.6	347 ± 15	0.17	0.9	3.0
$t\bar{t}H$	17	1.19 ± 0.13	1.4 ± 0.7	15.1 ± 2.2	0.36	9.2	3.2

Calculated in the 120-130GeV region
Major sensitive ones are VBF, ggF 2-jet and 1-jet categories

Categorization Performance (2)

Category	ggF	VBF	WH	ZH	$t\bar{t}H$
VBF Very High	6.6%	93.3%	0.0%	0.0%	0.0%
VBF High	12.8%	87.1%	0.0%	0.0%	0.0%
VBF Medium	21.3%	78.5%	0.1%	0.1%	0.0%
VBF Low	34.8%	64.8%	0.2%	0.2%	0.0%
2-jet Very High	82.0%	15.7%	1.2%	1.0%	0.2%
2-jet High	79.3%	16.0%	2.7%	1.8%	0.3%
2-jet Medium	80.7%	10.4%	5.4%	3.0%	0.5%
2-jet Low	78.2%	6.6%	8.8%	4.9%	1.5%
1-jet Very High	78.2%	21.2%	0.3%	0.3%	0.0%
1-jet High	88.2%	10.4%	0.9%	0.6%	0.0%
1-jet Medium	91.4%	6.1%	1.6%	0.9%	0.0%
1-jet Low	92.4%	3.8%	2.6%	1.2%	0.0%
0-jet Very High	94.1%	2.5%	1.4%	2.0%	0.0%
0-jet High	98.3%	1.0%	0.4%	0.3%	0.0%
0-jet Medium	99.1%	0.6%	0.2%	0.1%	0.0%
0-jet Low	99.5%	0.3%	0.1%	0.1%	0.0%
VH4L	0.0%	0.0%	0.1%	99.5%	0.4%
VH3LH	0.3%	0.1%	96.9%	2.6%	0.1%
VH3LM	4.2%	1.0%	80.8%	8.6%	5.3%
$t\bar{t}H$	0.1%	0.0%	1.5%	0.4%	98.0%

- Signal decomposition by production mode in each category
- The categories show high purity in their targeted production modes

H→μμ: Background Model

- A "core function" multiplied by an "empirical function" is used to model the background shape
  - Core function is a LO DY line-shape convoluted with a Gaussian function mimicking detector mass resolution effects
  - Empirical function is used to correct for distortions of the mass shape and smaller background
    - Power law function: $m_{\mu\mu}^{(a_0+a_1 m_{\mu\mu}+a_2 m_{\mu\mu}^2+\ldots+a_N m_{\mu\mu}^N)}$
    - Epoly function: $\exp(a_1 m_{\mu\mu} + a_2 m_{\mu\mu}^2 + \ldots + a_N m_{\mu\mu}^N)$
- Spurious signal (SS) uncertainty: derived by using S+B PDF to fit the pure background templates
  - Fast-simulation DY used for ggF/VBF categories, while full-sim non-DY bkg. samples used for VH/ttH categories

Background Function in Each Category

Category	Empirical Function	max(SS/ δS)[%]	max(SS/S_{SM})[%]
VBF Very High	Epoly1	-20.3	-34.8
VBF High	Power0	11.7	20.0
VBF Medium	Power0	8.5	16.4
VBF Low	Power0	11.2	2.4
2-jet Very High	Power1	-13.3	-34.5
2-jet High	Epoly2	-19.8	-41.2
2-jet Medium	Power1	19.8	40.9
2-jet Low	Epoly3	2.1	8.0
1-jet Very High	Epoly2	21.9	-53.4
1-jet High	Epoly2	-7.8	-18.5
1-jet Medium	Power1	4.2	7.9
1-jet Low	Power1	17.3	51.5
0-jet Very High	Power1	19.2	50.9
0-jet High	Power1	-19.4	43.5
0-jet Medium	Power1	25.8	69.4
0-jet Low	Epoly3	-20.8	-100.4
VH4L	Power1	20.7	230
VH3LH	Epoly2	36.9	210
VH3LM	Epoly3	33.6	276
ttH	Power0	32.2	117

- All functions pass the pre-defined selection criteria with SS values under control
- Chosen functions are typically with less degree of freedom comparing with EPS due to improved procedure

Systematic Uncertainties on Signals

- Theory uncertainties:
  - Branching ratio, QCD scale and PDF uncertainties on all production modes
  - Underlying event/Parton shower uncertainties on ggF/VBF
  - Heavy flavor uncertainty: 100% on ggF, VBF, and VH yields only in ttH category
- Experimental uncertainties:
  - Muon momentum scale, resolution, and efficiencies
  - Electron/photon scale and resolution
  - Jet energy scale/resolution, flavor tagging, quark-gluon tagging and E_T^{miss}
  - Luminosity, pileup reweighting, Run 1 LHC Higgs mass measurement uncertainty

Inclusive $m_{\mu\mu}$ Spectra

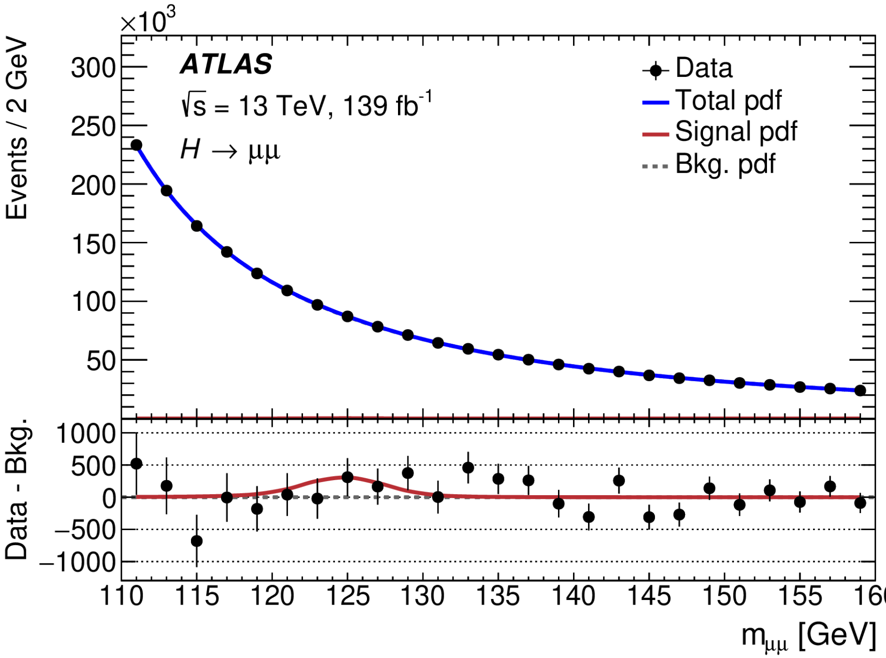

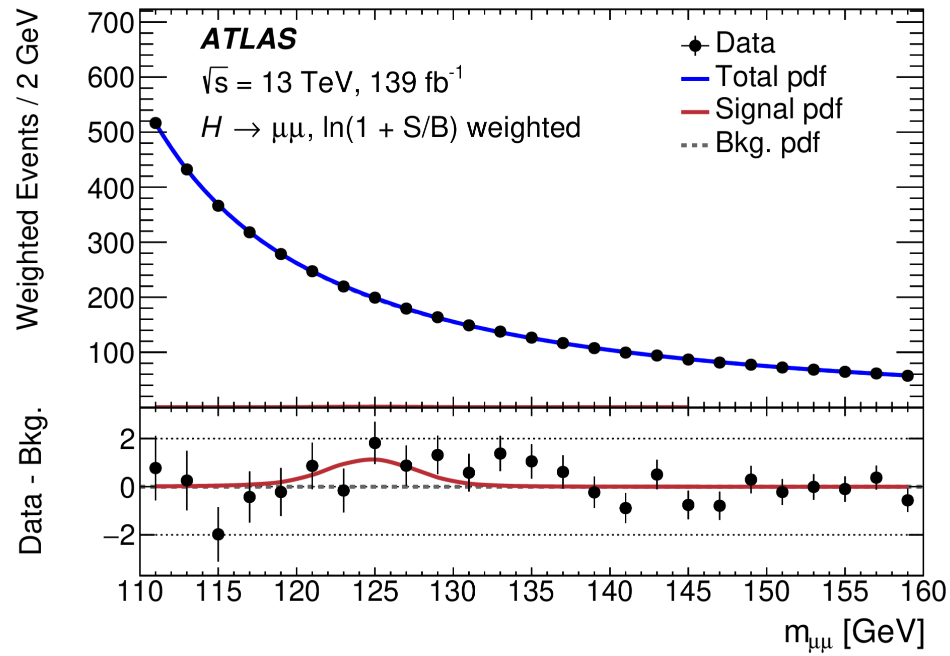

For figure on the right, events and PDFs are weighted by ln(1+S/B) of each category, where S and B are calculated within 120-130 GeV mass window

H→μμ: Results

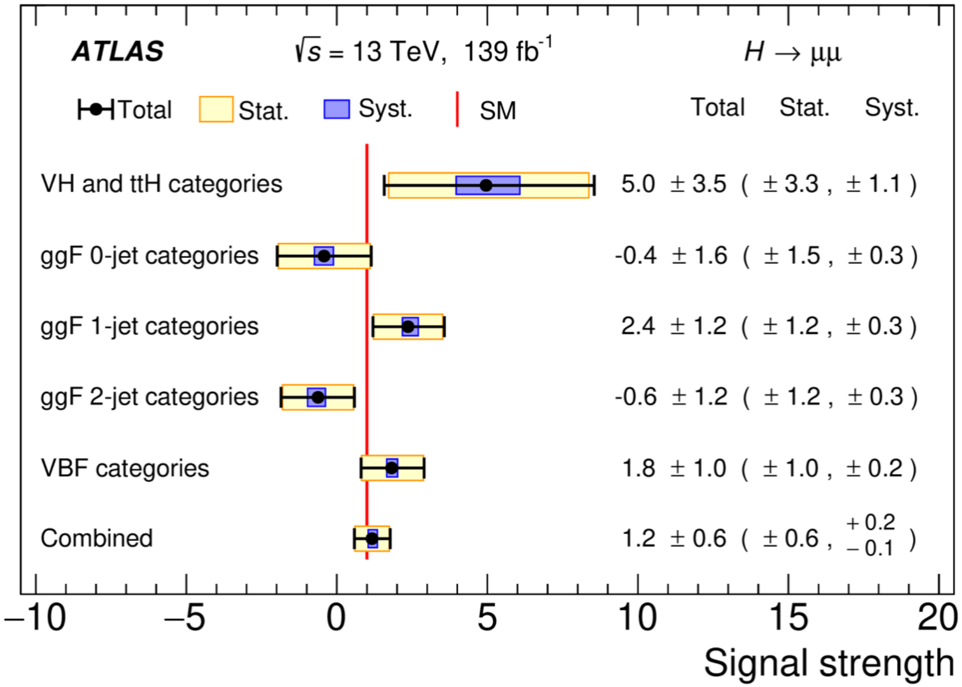

- Measured signal strengths for five groups of categories
- Results are consistent with the SM prediction
- Compatibility between the signal strengths in the five groups is 20%

Display for a VBF (H→μμ)-Like Event

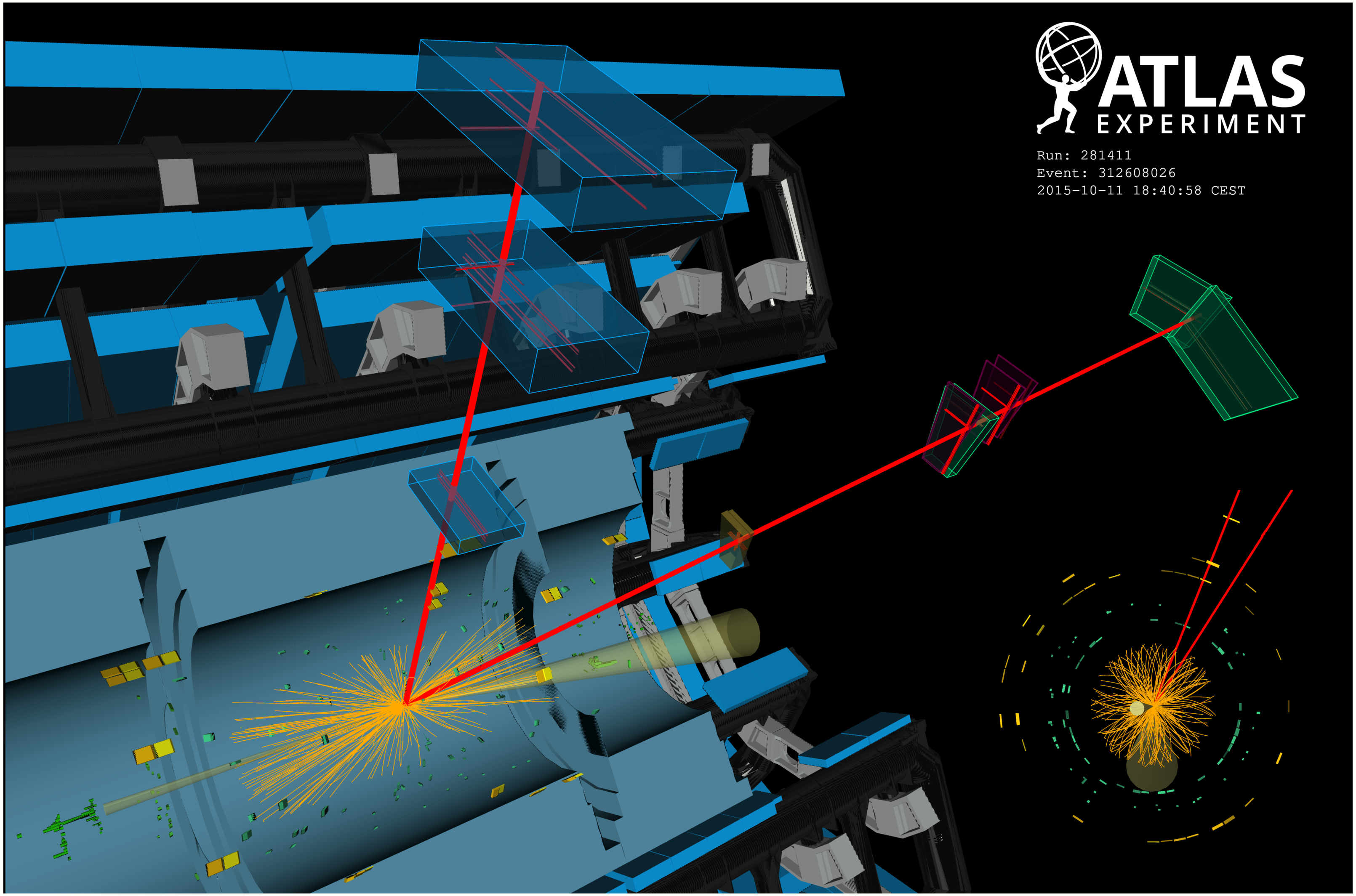

- Higgs trilinear self-coupling (κ_λ) can be directly probed via HH

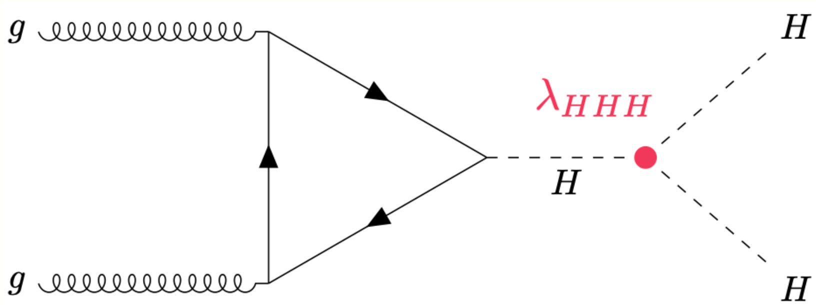

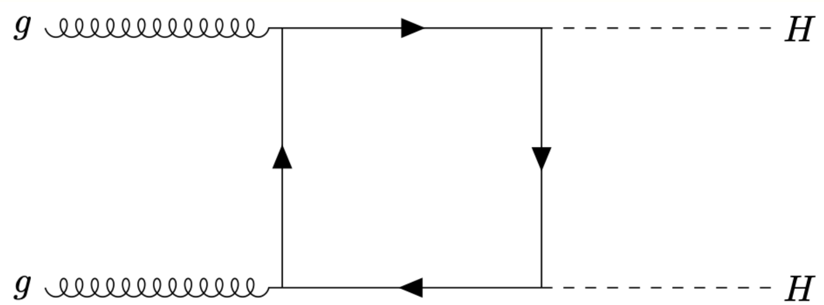

- κ_λ also can be constrained through NLO EW correction of single Higgs processes

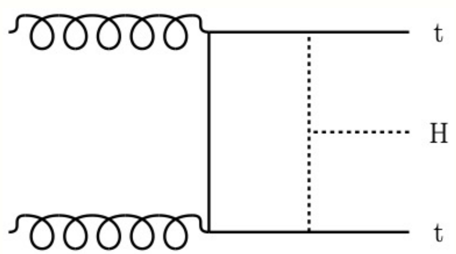

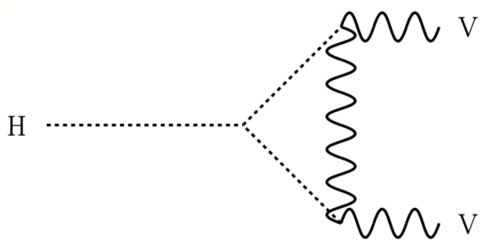

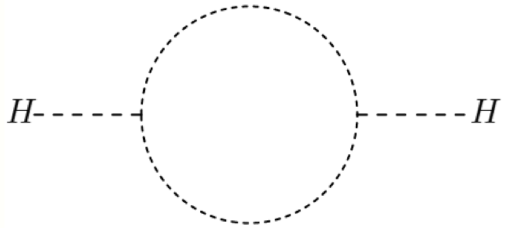

- ggF HH cross section depends on κ_λ and κ_t

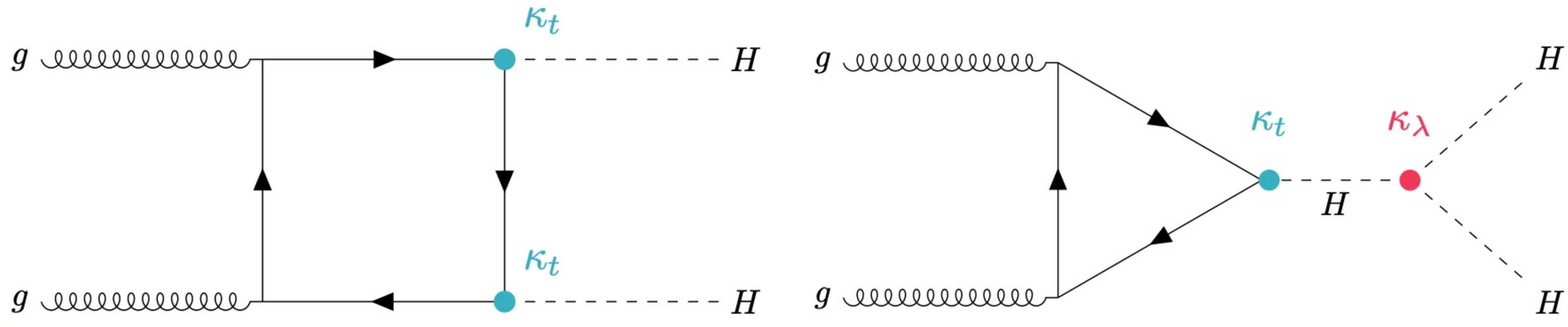

- Any (κ_λ , κ_t) can be obtained via a linear combination of three basis samples at different κ_λ values with κ_t = 1

$$\text{sample}(\kappa_\lambda, \kappa_t) = \kappa_t^2 \left[\left(\kappa_t^2 + \frac{\kappa_\lambda^2}{20} - \frac{399}{380} \kappa_\lambda \kappa_t \right) \cdot \text{sample}(0,1) + \left(\frac{40}{38} \kappa_\lambda \kappa_t - \frac{2}{38} \kappa_\lambda^2 \right) \cdot \text{sample}(1,1) + \left(\frac{\kappa_\lambda^2 - \kappa_\lambda \kappa_t}{380} \right) \cdot \text{sample}(20,1) \right]$$

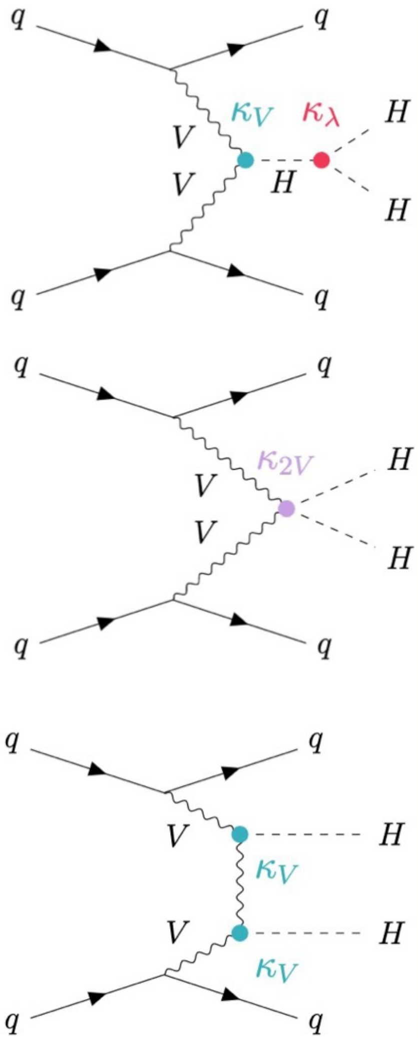

- VBF HH XS depends on κ_{2V}, κ_λ and κ_V
- A linear combination of 6 samples with different (κ_{2V}, κ_λ, κ_V) values
- Rank 1 basis used

$$\left(\frac{\kappa_{2V}^2}{5} - \frac{\kappa_{2V}\kappa_V^2}{5} - \frac{\kappa_{2V}\kappa_V\kappa_\lambda}{10} + \frac{\kappa_V^3\kappa_\lambda}{10}\right) \times \sigma(3, 1, 1)+$$
$$\left(\frac{4\kappa_{2V}^2}{5} - \frac{4\kappa_{2V}\kappa_V^2}{5} - \frac{12\kappa_{2V}\kappa_V\kappa_\lambda}{5} + \frac{12\kappa_V^3\kappa_\lambda}{5}\right) \times \sigma\left(\frac{1}{2}, 1, 1\right)+$$
$$\left(-\frac{5\kappa_{2V}\kappa_V^2}{4} + \frac{5\kappa_{2V}\kappa_V\kappa_\lambda}{4} + \frac{\kappa_V^3\kappa_\lambda}{8} - \frac{\kappa_V^2\kappa_\lambda^2}{8}\right) \times \sigma(1, 2, 1)+$$
$$\left(-\kappa_{2V}\kappa_V^2 + \kappa_{2V}\kappa_V\kappa_\lambda + \kappa_V^4 - \kappa_V^3\kappa_\lambda\right) \times \sigma(0, 0, 1)+$$
$$\left(\frac{\kappa_{2V}\kappa_V^2}{36} - \frac{\kappa_{2V}\kappa_V\kappa_\lambda}{36} - \frac{\kappa_V^3\kappa_\lambda}{72} + \frac{\kappa_V^2\kappa_\lambda^2}{72}\right) \times \sigma(1, 10, 1)+$$
$$\left(-\kappa_{2V}^2 + \frac{29\kappa_{2V}\kappa_V^2}{9} + \frac{5\kappa_{2V}\kappa_V\kappa_\lambda}{18} - \frac{29\kappa_V^3\kappa_\lambda}{18} + \frac{\kappa_V^2\kappa_\lambda^2}{9}\right) \times \sigma(1, 1, 1)$$

Triggers

- $\tau_{lep}\tau_{had}$ channel
  - SLT (single e/μ trigger): priority is given
    - Lowest un-prescaled, isolated with p_T 20-26 GeV
    - e: 60, 120, 140, 300 GeV supplementary non-isolated triggers
    - μ: 50 and 60 GeV supplementary non-isolated triggers
  - LTT (lepton+τ trigger): checked if not passing SLT
    - 14 (17) GeV μ (e) + 25/35 GeV medium τ_{had}
- $\tau_{had}\tau_{had}$ channel
  - STT (single τ_{had} trigger): priority is given
    - 80, 125 and 160 GeV medium τ_{had}
  - DTT (di-τ_{had} trigger): checked if not passing STT
    - 2 medium τ_{had} with p_T > 35 (25) GeV + 25 GeV L1 jet

Selection Criteria

$\tau_{\mathrm{had}}\tau_{\mathrm{had}}$ category		$\tau_{\mathrm{lep}}\tau_{\mathrm{had}}$ categories	
STT	DTT	SLT	LTT
	e/μ selection		
No loose e/μ with $p_{\mathrm{T}} > 7$ GeV		Exactly one tight e or medium μ	
		$p_{\mathrm{T}}^{e} > 25, 27$ GeV	18 GeV $< p_{\mathrm{T}}^{e} <$ SLT cut
		$p_{\mathrm{T}}^{\mu} > 21, 27$ GeV	15 GeV $< p_{\mathrm{T}}^{\mu} <$ SLT cut
		$\lvert\eta^{e}\rvert < 2.47$, not $1.37 < \lvert\eta^{e}\rvert < 1.52$	
		$\lvert\eta^{\mu}\rvert < 2.7$	
	$\tau_{\text{had-vis}}$ selection		
Two loose $\tau_{\text{had-vis}}$		One loose $\tau_{\text{had-vis}}$	
$\lvert\eta\rvert < 2.5$		$\lvert\eta\rvert < 2.3$	
$p_{\mathrm{T}} > 100, 140, 180$ (25) GeV	$p_{\mathrm{T}} > 40$ (30) GeV	$p_{\mathrm{T}} > 20$ GeV	$p_{\mathrm{T}} > 30$ GeV
	Jet selection		
	≥ 2 jets with $\lvert\eta\rvert < 2.5$		
$p_{\mathrm{T}} > 45$ (20) GeV	Trigger dependent	$p_{\mathrm{T}} > 45$ (20) GeV	Trigger dependent
	Event-level selection		
	Trigger requirements passed		
	Collision vertex reconstructed		
	$m_{\tau\tau}^{\mathrm{MMC}} > 60$ GeV		
	Opposite-sign electric charges of $e/\mu/\tau_{\text{had-vis}}$ and $\tau_{\text{had-vis}}$		
	Exactly two b-tagged jets		
		$m_{bb} < 150$ GeV	

Signal Acceptance × Efficiency

- The acceptance times efficiency for the non-resonant ggF+VBF evaluated w.r.t. targeted τ decay modes
  - $\tau_{had}\tau_{had}$: 4.0%, $\tau_{lep}\tau_{had}$ SLT: 4.0%, $\tau_{lep}\tau_{had}$ LTT: 1.0%
- Around factor 2 improvement on signal acceptance compared with previous publication*
- Driven by improved reconstruction and identification of τ_{had} and b-jets**

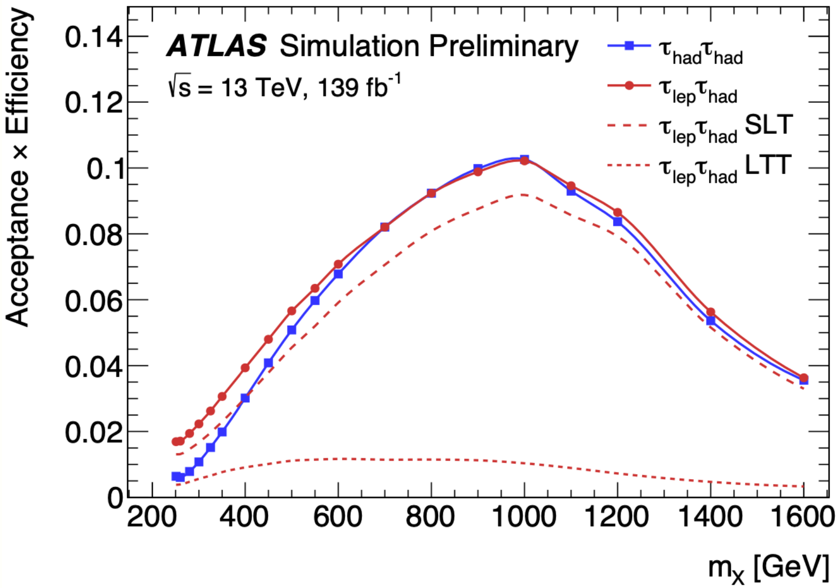

*Phys. Rev. Lett. 121, 191801

**ATL-PHYS-PUB-2017-003, ATL-PHYS-PUB-2017-013, ATL-PHYS-PUB-2019-033

HL-LHC Projection

Uncertainty scenario	Significance [σ] $b\bar{b}\gamma\gamma$	$b\bar{b}\tau^+\tau^-$	Combination	Combined signal strength precision [%]
No syst. unc.	2.3	4.0	4.6	$-23/+23$
Baseline	2.2	2.8	3.2	$-31/+34$
Theoretical unc. halved	1.1	1.7	2.0	$-49/+51$
Run 2 syst. unc.	1.1	1.5	1.7	$-57/+68$

Uncertainty scenario	Likelihood scan 1 σ CI	Likelihood scan 2 σ CI
No syst. unc.	[0.6, 1.5]	[0.3, 2.1]
Baseline	[0.5, 1.6]	[0.0, 2.7]
Theoretical unc. halved	[0.2, 2.2]	[−0.4, 5.6]
Run 2 syst. unc.	[0.1, 2.5]	[−0.7, 5.7]

ATL-PHYS-PUB-2022-005

κ_λ-dependence of XS and BR

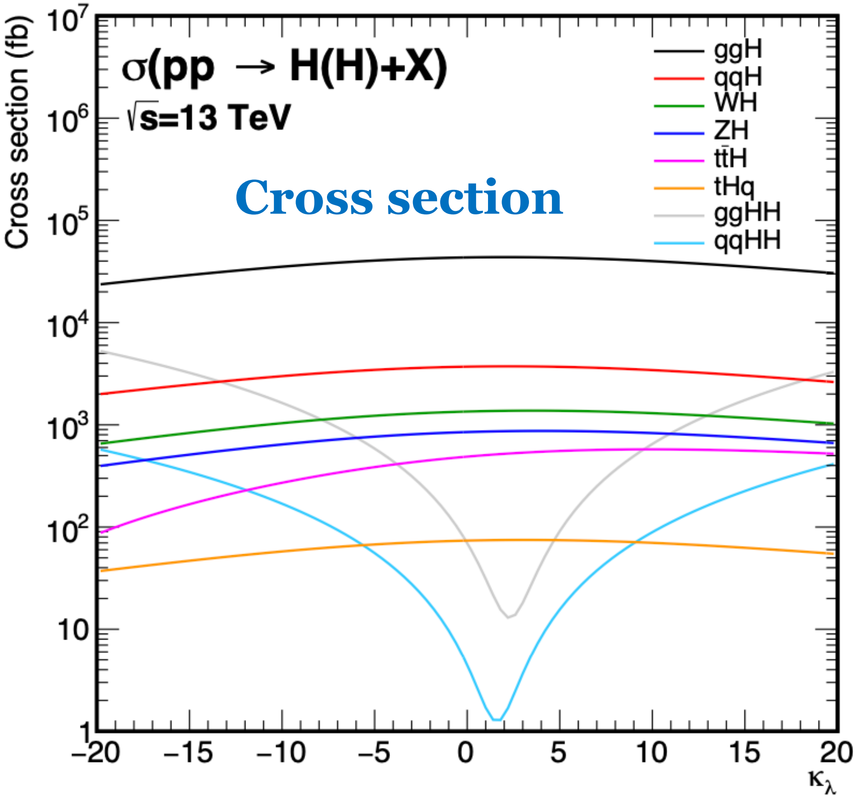

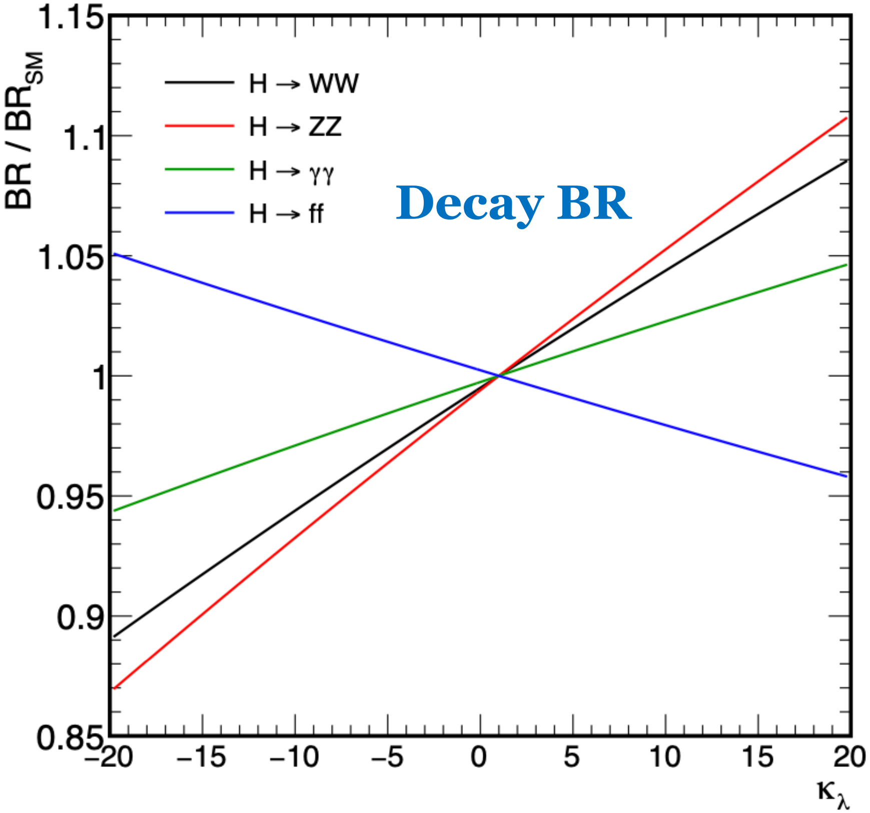

Flavor Tagging Improvement

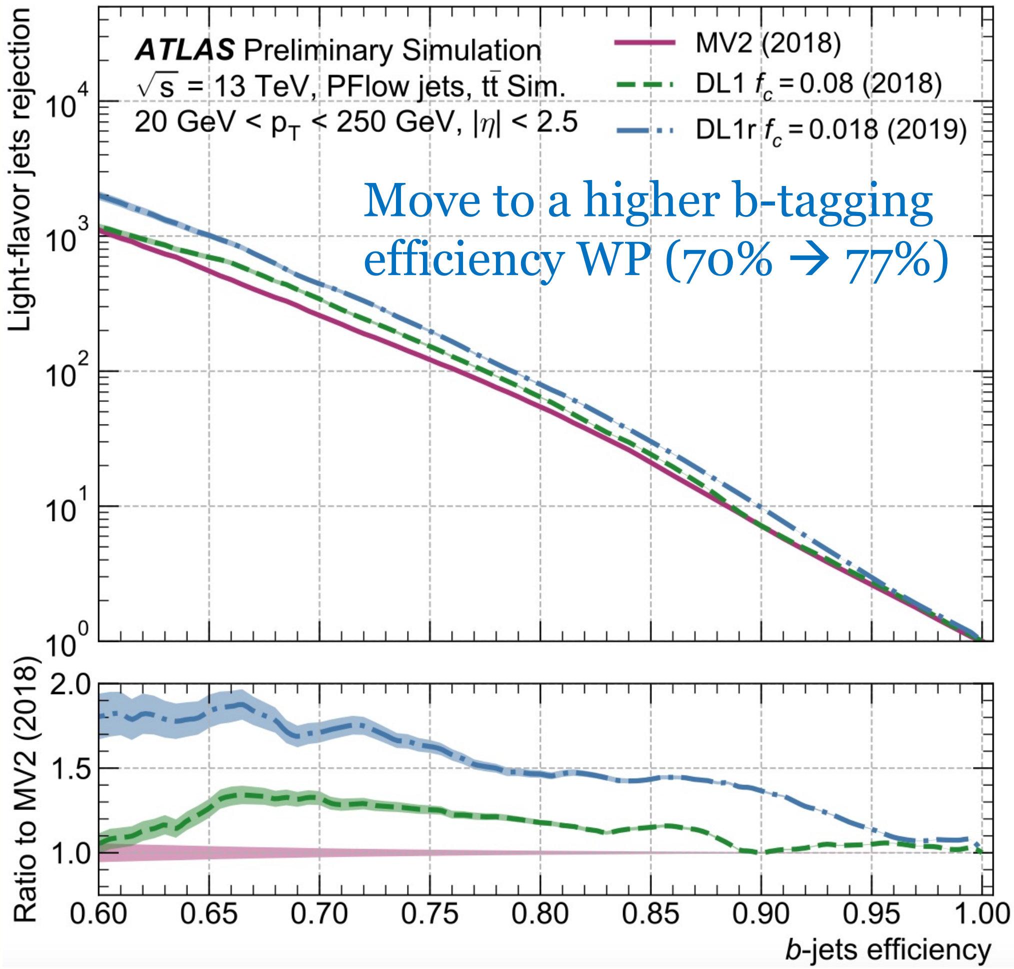

Move to a higher b-tagging efficiency WP (70% → 77%)

Likelihood-based calibration provides >2x reduction in uncertainties

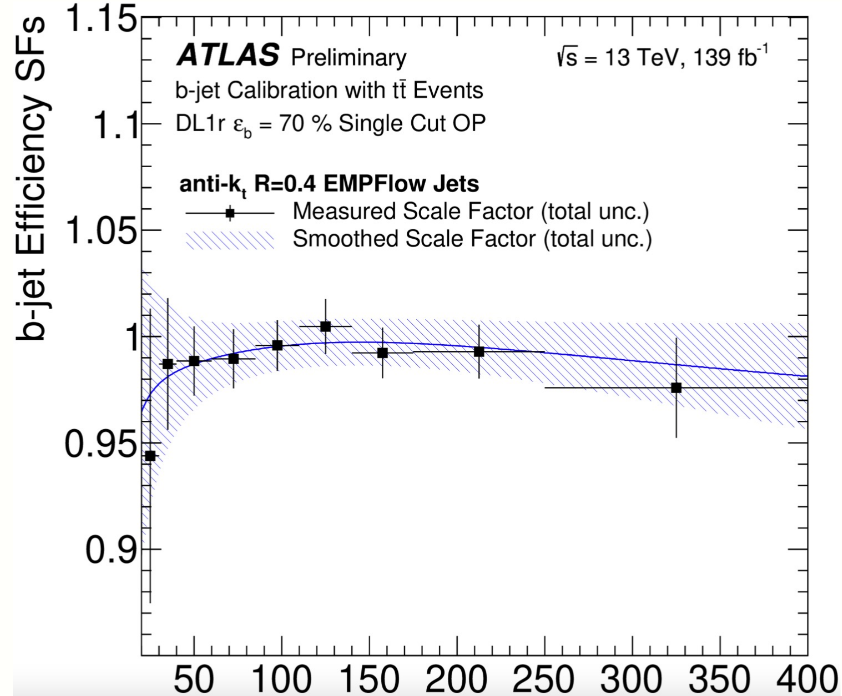

τ Identification Improvement

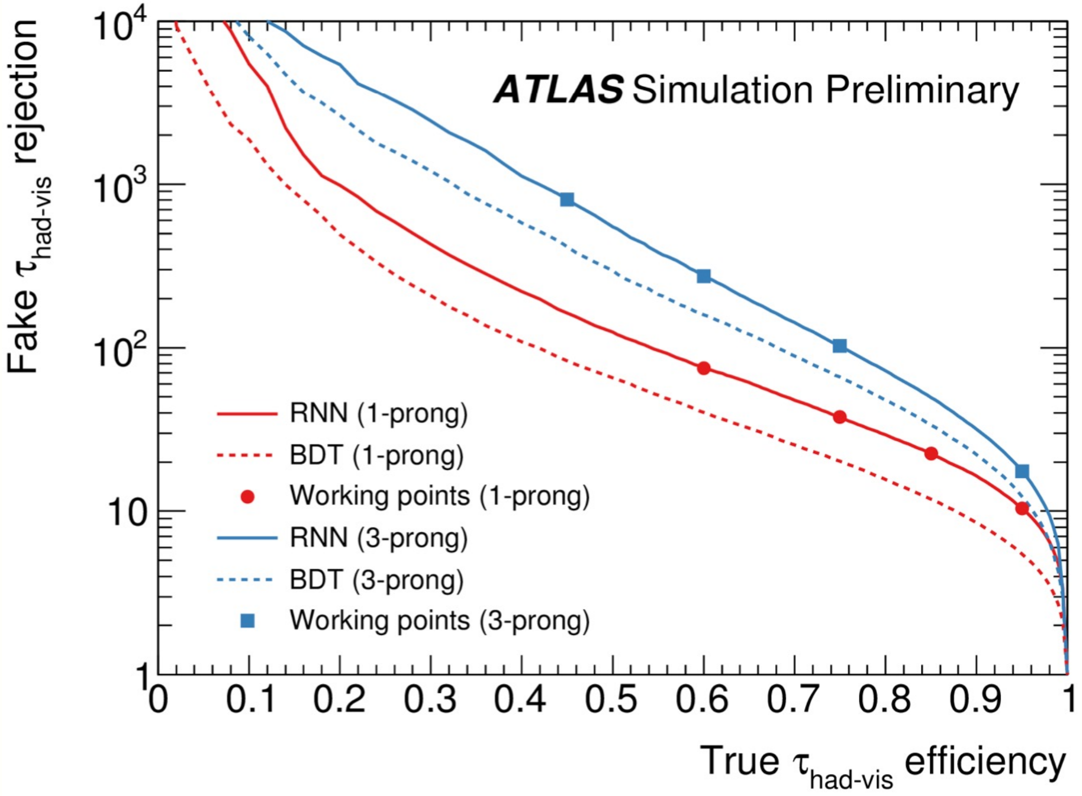

RNN ID shows 2x improvement compared with BDT

Moved from “medium” to “loose” WP

Per-tau efficiency:

1-prong: 75% → 85%

3-prong: 60% → 75%

Variable	$\tau_{\rm had}\tau_{\rm had}$	$\tau_{\rm lep}\tau_{\rm had}$ SLT	$\tau_{\rm lep}\tau_{\rm had}$ LTT
m_{HH}	✓	✓	✓
$m_{\tau\tau}^{\rm MMC}$	✓	✓	✓
m_{bb}	✓	✓	✓
$\Delta R(\tau,\tau)$	✓	✓	✓
$\Delta R(b,b)$	✓	✓	
$\Delta p_{\rm T}(\ell,\tau)$		✓	✓
Sub-leading b-tagged jet $p_{\rm T}$		✓	
$m_{\rm T}^{W}$		✓	
$E_{\rm T}^{\rm miss}$		✓	
$\mathbf{p}_{\rm T}^{\rm miss}$ ϕ centrality		✓	
$\Delta\phi(\ell\tau, bb)$		✓	
$\Delta\phi(\ell, \mathbf{p}_{\rm T}^{\rm miss})$			✓
$\Delta\phi(\ell\tau, \mathbf{p}_{\rm T}^{\rm miss})$			✓
$S_{\rm T}$			✓

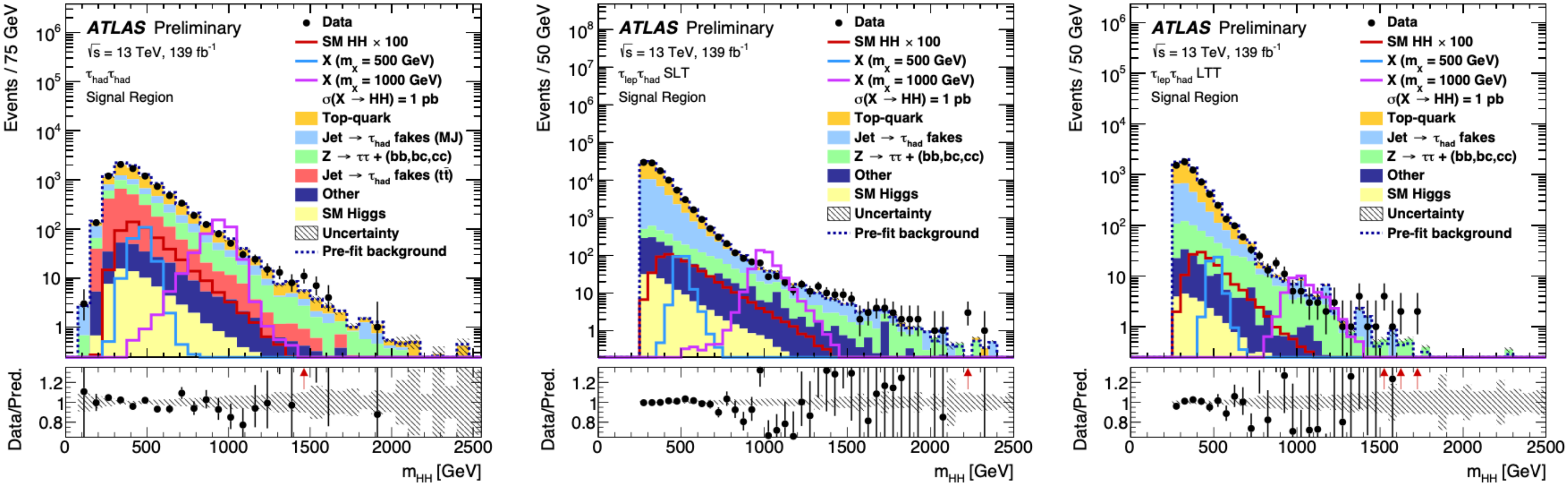

ATLAS Preliminary
√s = 13 TeV, 139 fb⁻¹
τhadτhad
Signal Region
Data
SM HH × 100
X (mX = 500 GeV)
X (mX = 1000 GeV)
σ(X → HH) = 1 pb
Top-quark
Jet → τhad fakes (MJ)
Z → ττ + (bb,bc,cc)
Jet → τhad fakes (tt̄)
Other
SM Higgs
Uncertainty
Pre-fit background
Events / 75 GeV
Data/Pred.
mHH [GeV]
ATLAS Preliminary
√s = 13 TeV, 139 fb⁻¹
τlepτhad SLT
Signal Region
Data
SM HH × 100
X (mX = 500 GeV)
X (mX = 1000 GeV)
σ(X → HH) = 1 pb
Top-quark
Jet → τhad fakes
Z → ττ + (bb,bc,cc)
Other
SM Higgs
Uncertainty
Pre-fit background
Events / 50 GeV
Data/Pred.
mHH [GeV]
ATLAS Preliminary
√s = 13 TeV, 139 fb⁻¹
τlepτhad LTT
Signal Region
Data
SM HH × 100
X (mX = 500 GeV)
X (mX = 1000 GeV)
σ(X → HH) = 1 pb
Top-quark
Jet → τhad fakes
Z → ττ + (bb,bc,cc)
Other
SM Higgs
Uncertainty
Pre-fit background
Events / 50 GeV
Data/Pred.
mHH [GeV]

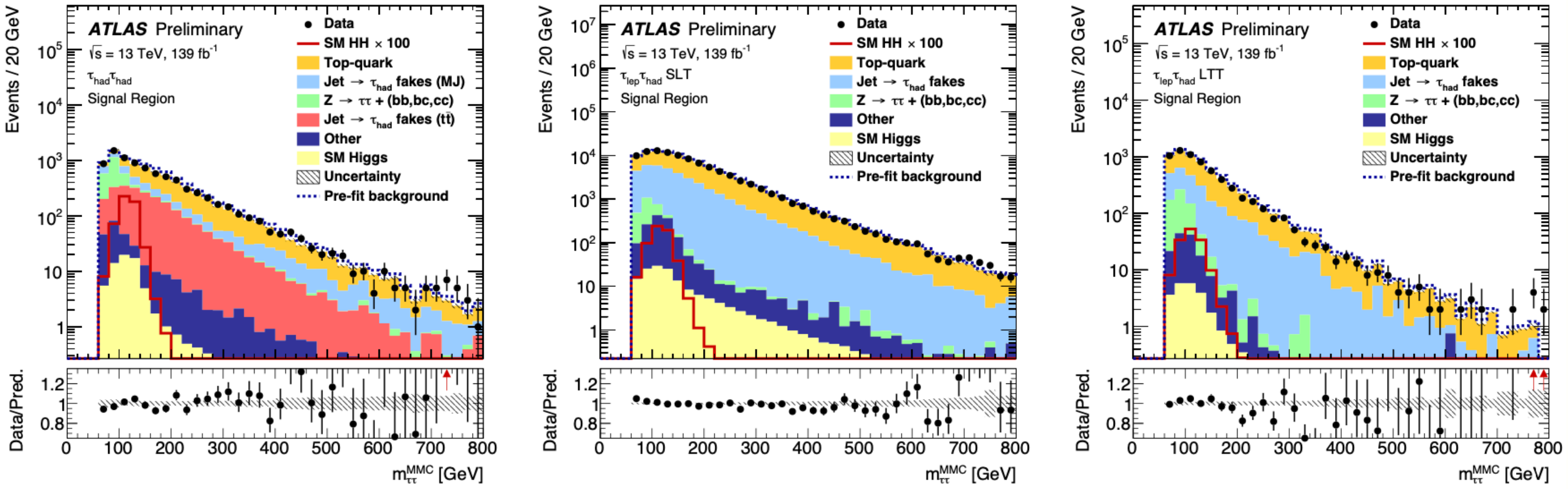
ATLAS Preliminary
√s = 13 TeV, 139 fb-1
τhadτhad
Signal Region
Data
SM HH × 100
Top-quark
Jet → τhad fakes (MJ)
Z → ττ + (bb,bc,cc)
Jet → τhad fakes (tt̄)
Other
SM Higgs
Uncertainty
Pre-fit background
Events / 20 GeV
Data/Pred.
m_ττ^MMC [GeV]
ATLAS Preliminary
√s = 13 TeV, 139 fb-1
τlepτhad SLT
Signal Region
Data
SM HH × 100
Top-quark
Jet → τhad fakes
Z → ττ + (bb,bc,cc)
Other
SM Higgs
Uncertainty
Pre-fit background
Events / 20 GeV
Data/Pred.
m_ττ^MMC [GeV]
ATLAS Preliminary
√s = 13 TeV, 139 fb-1
τlepτhad LTT
Signal Region
Data
SM HH × 100
Top-quark
Jet → τhad fakes
Z → ττ + (bb,bc,cc)
Other
SM Higgs
Uncertainty
Pre-fit background
Events / 20 GeV
Data/Pred.
m_ττ^MMC [GeV]

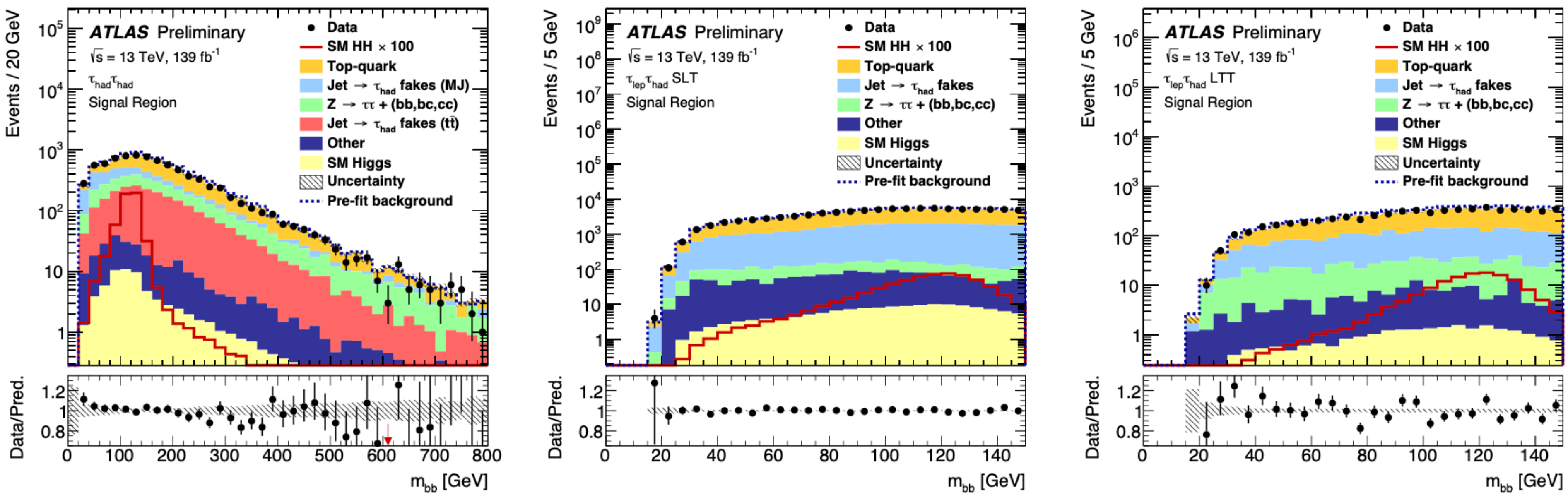
ATLAS Preliminary
√s = 13 TeV, 139 fb⁻¹
τhadτhad
Signal Region
Data
SM HH × 100
Top-quark
Jet → τhad fakes (MJ)
Z → ττ + (bb,bc,cc)
Jet → τhad fakes (tt̄)
Other
SM Higgs
Uncertainty
Pre-fit background
Events / 20 GeV
Data/Pred.
mbb [GeV]
ATLAS Preliminary
√s = 13 TeV, 139 fb⁻¹
τlepτhad SLT
Signal Region
Data
SM HH × 100
Top-quark
Jet → τhad fakes
Z → ττ + (bb,bc,cc)
Other
SM Higgs
Uncertainty
Pre-fit background
Events / 5 GeV
Data/Pred.
mbb [GeV]
ATLAS Preliminary
√s = 13 TeV, 139 fb⁻¹
τlepτhad LTT
Signal Region
Data
SM HH × 100
Top-quark
Jet → τhad fakes
Z → ττ + (bb,bc,cc)
Other
SM Higgs
Uncertainty
Pre-fit background
Events / 5 GeV
Data/Pred.
mbb [GeV]

New Small Wheel

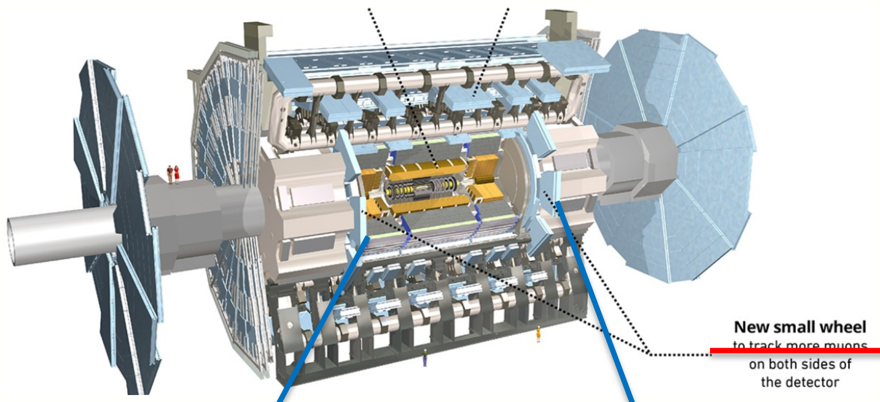

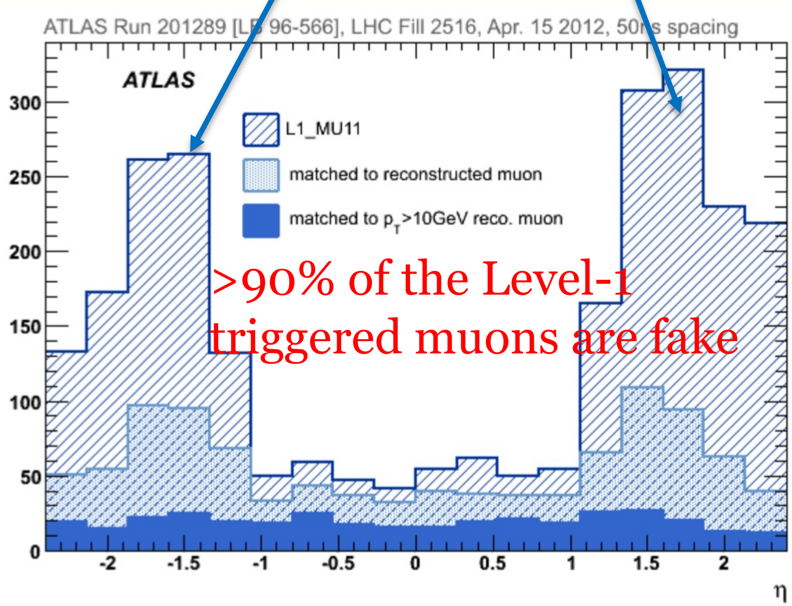

Two types of technology adopted for triggering and precision tracking: small-strip Thin Gap Chambers (sTGC) and Micromegas detectors (MM)

sTGC Trigger Chain

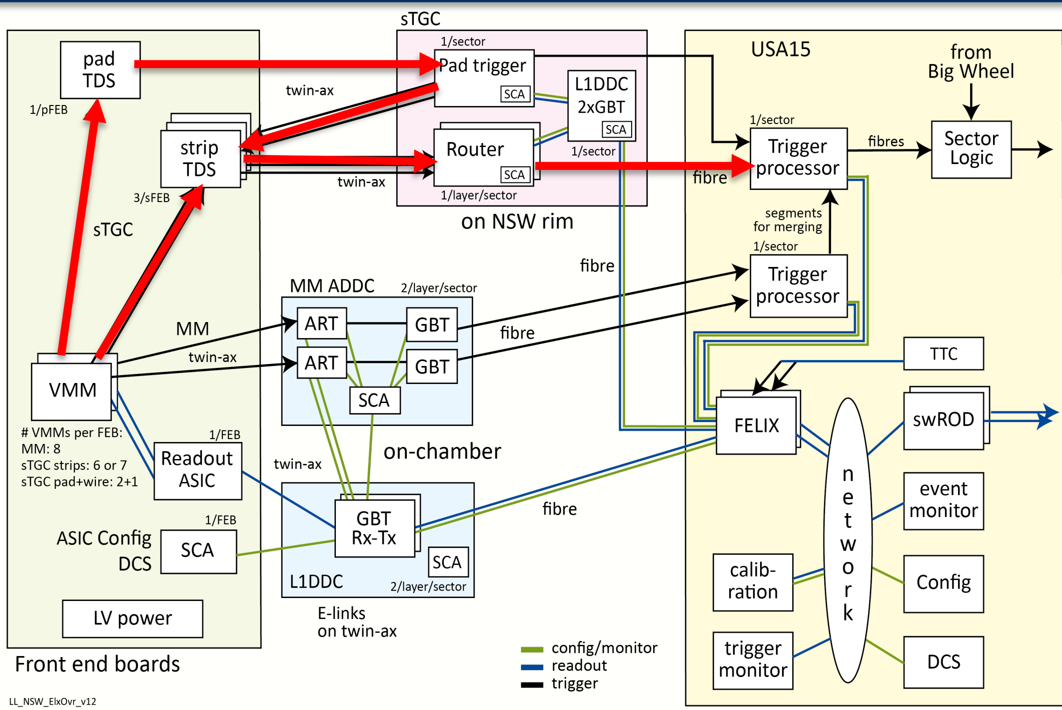

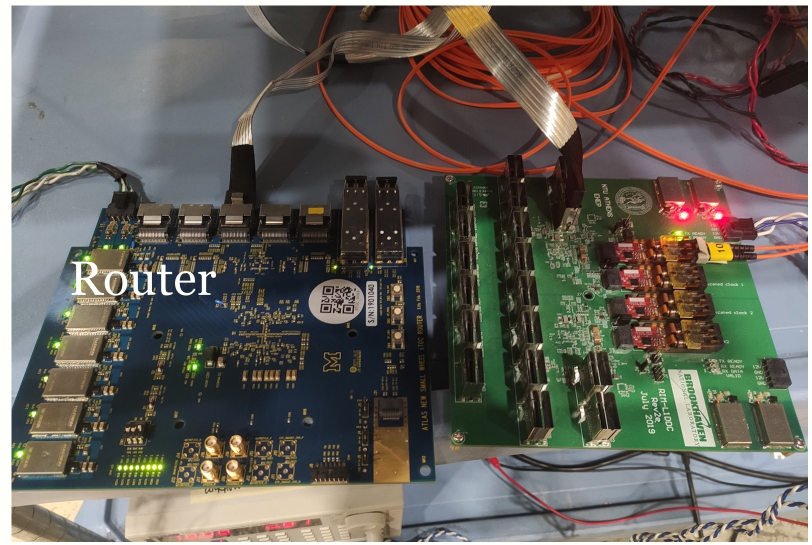

Photo took from a bench test

Focusing on the trigger chain (red lines) work for sTGC, and responsible for the test/commissioning/debugging for the router boards (in total 256 router boards are assembled for two sides of the detector)